

The Possible Protective Effect of Mesenchymal Stem Cells and Alfacalcidol in Cisplatin Induced Acute Kidney Injury in Adult Male Albino Rats

Melad N. Kelada^{1,2}, Abdelghany H. Abdelghany¹, Dina S. Dawood¹, Walaa Omar³, Marwa M. Mady^{1,4}

¹ Department of Human Anatomy and Embryology, Faculty of Medicine, Alexandria University, Alexandria, Egypt

² Department of Human Anatomy and Embryology, Beirut Arab University, Beirut, Lebanon

³ Histology and Cell Biology Department, Faculty of Medicine, Alexandria University, Alexandria, Egypt

⁴ Biomedical Sciences Department, College of Medicine, Gulf Medical University (GMU), Ajman, UAE

SUMMARY

Cisplatin is one of the most effective chemotherapeutic agents, but nephrotoxicity is its major hazard. This study aimed to evaluate the possible protective effects of mesenchymal stem cell and alfacalcidol in ameliorating cisplatin-induced nephrotoxicity in albino rats. Five young male albino rats were utilized to obtain BM-MSCs. Forty adult male albino rats were divided into: Group I, n=8: (control), Group II, n=8 (cisplatin): received cisplatin (6.5 mg/kg) IP as a single dose on day 0, Group III, n=24 (treatment): subdivided into: subgroup IIIa (Alfacalcidol): received 50 ng/kg/day alfacalcidol oral daily dose for 5 days, then received cisplatin (as group II), then continued alfacalcidol for another 5 days, Subgroup IIIb (Alfacalcidol) (BM-MSCs): received cisplatin (as group II) on day 0, then received BM-MSCs suspension injected into the tail vein after cisplatin, in a dose of 2×10^6 in 0.5 ml PBS/rat, Subgroup IIIc: (BM-MSCs and alfacalcidol): received 50 ng/kg/day alfacalcidol orally daily dose for 5 days, then cisplatin (as

group II) then BM-MSCs suspension injected into the tail vein, in a dose of 2×10^6 in 0.5 ml PBS/rat one day after cisplatin then continued alfacalcidol for another 5 days. Blood urea and serum creatinine were measured, and kidneys were processed for histological, immunohistochemical and morphometric studies.

Combined alfacalcidol-and-BM-MSCs-treated group IIIc exhibited marked improvement in histological structure of the kidney and renal functions. Combined treatment of alfacalcidol with BM-MSCs may represent a suitable modality in alleviating cisplatin-induced acute kidney injury than using each modality alone.

Key words: AKI – BM-MSCs – Alfacalcidol – Cisplatin – Albino rats

INTRODUCTION

The kidneys are the primary organs impacted by toxic metabolites and medications that are eliminated (Mazher et al., 2021). Drug-induced

Corresponding author:

Dr. Melad N. Kelada, Associate professor. Anatomy and Embryology Department, Faculty of Medicine. Alexandria University. Associate professor of Human Anatomy and Embryology, Faculty of medicine, Beirut Arab University, Beirut, Lebanon. Phone: +961 03 715 764. Mobile: +201002470484. E-mail: melad.bushra@alexmed.edu.eg / m.kelada@bau.edu.lb - ORCID: 0000-0001-9065-4523

Submitted: August 17, 2025. **Accepted:** October 25, 2025

<https://doi.org/10.52083/JBG07788>

nephrotoxicity involves kidney injury caused by medications. The presentation varies from an acute or chronic injury to nephrotic syndrome and electrolyte disturbances, which are linked to glomerular and tubular damage, respectively (Abd El Zaher et al., 2017). Acute kidney injury (AKI) is a clinical syndrome manifested by rapid decline in kidney function. It is a condition caused by a number of different insults, with a mortality rate ranging from 30 to 80%. Up to 25% of all instances of acute renal damage can be caused by drugs (Abd El Zaher et al., 2017).

Cisplatin is one of the most effective chemotherapeutic agents, and it is widely used in the treatment of a variety of human tumors. It mediates its tumoricidal effects via a number of different cytotoxic mechanisms. While cisplatin is mostly recognized for its ability to destroy DNA, it also disrupts cytoplasmic organelles, especially the mitochondria and endoplasmic reticulum. Moreover, it triggers apoptotic pathways and causes inflammation and oxidative stress (Yamamoto et al., 2013). One of its dose-limiting toxicities is its effect on the kidney. This includes acute kidney injury, which affects around one-third of patients (Bennis et al., 2014). For this reason, cisplatin was selected in the present study to cause AKI (Abd El Zaher et al., 2017).

The pathophysiology of AKI is complex, and involves tubular and vascular damage and inflammatory reactions. Current therapies of AKI mainly include supportive care, including renal replacement therapy. Despite these therapies, the five-year mortality rate for patients with AKI remains over 50%. Hence, new therapeutic interventions and strategies for improving survival outcome for patients with AKI are needed (Zaahkoug et al., 2015).

Alfacalcidol is a widely used active vitamin-D compound, especially in clinical nephrology, because it does not require enzymatic activation by the kidneys (Fouad et al., 2010). It is a fat-soluble vitamin D, well absorbed orally in the presence of bile. It can also be given intravenously, has a short half-life (about 3 hours), and is metabolized and excreted mainly in the bile (Ali et al., 2018). Over the last few decades, it has become clear that vitamin-D deficiency has a direct correlation with

kidney disease (Hu et al., 2020; Mata-Miranda et al., 2019; Wu et al., 2021; Devine et al., 2003). Vitamin-D depletion contributes to AKI development by leading to upregulation of RAAS (Renin-Angiotensin-Aldosterone System) and to elevated mRNA expression of renal-vascular renin (Imberti et al., 2007).

One of the most important mechanisms underlying cisplatin nephrotoxicity is oxidative stress. This oxidative stress triggers apoptosis, inflammation and intracellular damage. In this case, administering an antioxidant such as alfacalcidol may be a good way to avoid cisplatin nephrotoxicity (Tolouian et al., 2023).

Mesenchymal stem cells (MSCs) are adult stem cells capable of self-renewal and multilineage differentiation. They are adherent spindle-shaped cells isolated from bone marrow, adipose tissue, umbilical cord, and other tissue sources showing multipotent differentiation characteristics *in vitro* (Maridas et al., 2018; Huang et al., 2015). Recently, MSCs are the preferred stem cells for cellular therapy of AKI. This is because they are able to differentiate into cells of mesenchymal and non-mesenchymal origin, ease of culture and *ex vivo* expansion, and anti-inflammatory, anti-apoptotic and immunosuppressive effects (Zaahkoug et al., 2015).

The current study aimed to assess the effects of bone-marrow-derived mesenchymal stem cells (BM-MSCs) and alfacalcidol treatment, alone or as a combined treatment to ameliorate cisplatin-induced nephrotoxicity and to restore renal structure and function in albino rats.

Although both vitamin D analogues and MSCs have separately shown renoprotective effects in models of acute kidney injury, the potential benefit of combining alfacalcidol with bone marrow-derived MSCs in cisplatin-induced nephrotoxicity has not been previously investigated. We hypothesized that alfacalcidol, through its antioxidant and anti-inflammatory properties, would complement the regenerative and immunomodulatory actions of MSCs, resulting in enhanced protection of renal structure and function.

MATERIALS AND METHODS

Experimental animals

Forty adult male albino rats, 6 weeks old, weighing 150-200 gm and five young male albino rats about 2 weeks old and weighing about 80 gm were purchased from and raised in the Animal House Center of Physiology Department, Faculty of Medicine, Alexandria University, Egypt. They were maintained under a 12 h dark/light cycle $22\pm 2^\circ\text{C}$ and $50\pm 10\%$ humidity.

Diet was administered following the Egyptian Institute of Nutrition (EIN) guides. The diet was composed of: Bran – cottonseed meal - yellow corn - molasses - limestone powder - table salt. It was obtained from Tanta Oil and Soap Company, Egypt. The animals were given food and water *ad libitum*.

The study protocol was approved by the Ethics Committee of the Faculty of Medicine, Alexandria University (IRB No: 00012098- FWA No: 00018699). Serial number 0106994. All animal experiments complied with ARRIVE guidelines and were carried out in accordance with the U.K. Animals (Scientific Procedures) Act, 1986 and associated guidelines, EU Directive 2010/63/EU for animal experiments.

Isolation of rat BM-MSCs

Five young male albino rats, 2 weeks old, were sacrificed to obtain MSCs from their long bones. The nucleated cells were isolated and cultured in complete culture medium supplemented with 1% penicillin-streptomycin, then were incubated in humidified carbon dioxide for 12 to 14 days. After third passage, BM-MSCs were assessed by flow cytometer and used for treatment.

Cell confluence in culture was estimated by visual inspection under an inverted phase-contrast microscope (Nikon TSM) equipped with digital camera (DCM 510) by comparing the cell-covered area with the total flask area, as routinely used for MSC cultures (Abo-Aziza and Zaki, 2017).

This was performed in the center of excellence in research for regenerative medicine and its applications (CERMA), Faculty of Medicine, Alexandria University, Alexandria, Egypt (Abd El Zaher et

al., 2017; Maridas et al., 2018; Huang et al., 2015).

Flow cytometric analysis of rat BM-MSCs

Flow cytometer was used to assess the phenotype of the third passage of MSCs by analyzing their specific surface antigen profile. Cultured cells were detached with 0.25% trypsin-EDTA solution, washed with PBS, and incubated (30 min, in the dark) with monoclonal PE-conjugated antibodies for CD44 and CD45 and FITC-conjugated antibodies for CD90. The cells were subsequently washed three times with PBS, resuspended in 500 μL FACS buffer. Cells were analyzed using a FACS flow cytometer running Cell Quest software (Becton Dickinson, USA) (Abd El Zaher et al., 2017; Nery et al., 2013). Forward scatter (FSC) correlates with cell size, while side scatter (SSC) reflects cell granularity. Cells were first visualized on FSC–SSC plots to identify the main BM-MSC population (gate R1). Aliquots of the same P3 cell suspension were then stained with either CD44-PE and analyzed as FSC/SSC versus CD44 (panels a,b) or CD90-FITC and CD45-PE, and analyzed as FSC/SSC versus CD90/CD45 (panels c,d).

Experimental Design

In this study, forty animals were randomly divided into three groups:

Group I (control, n=8): these were further subdivided randomly into two subgroups:

Subgroup Ia (n=4): where rats received standard diet and free access to water
Subgroup Ib (n=4): where rats received a single dose of sodium chloride (vehicle of cisplatin) intraperitoneal (IP) 0.9% (6.5 ml/kg body weight) (Abdelrahman et al., 2023).

Group II (cisplatin group, n=8): rats received cisplatin (6.5 mg/kg) IP as a single dose (Abdelrahman et al., 2023; Abd Elsamie et al., 2023).

Group III (treatment group, n=24): were randomly subdivided into three subgroups:

Subgroup IIIa: (Alfacalcidol treated subgroup, n=8): rats in this group received 50 ng/kg/day alfacalcidol orally as a daily dose by orogastric tube for 5 days before cisplatin injection. Then they received cisplatin in a dose and route similar to

group II. Then they continued alfacalcidol for another 5 days after cisplatin dose (Abd Elsamie et al., 2023; Moneim et al., 2019).

Subgroup IIIb: (BM-MSCs treated subgroup, n=8): rats received cisplatin in a dose and route similar to group II on day 0 then they received the BM-MSCs suspension one day after cisplatin injection. The BM-MSCs suspension was injected into the rat tail vein, in a dose of 2×10^6 in 0.5 ml PBS/rat (Abd El Zaher et al., 2017; LZ et al., 2013).

Subgroup IIIc: (BM-MSCs and alfacalcidol treated subgroup, n=8): rats received 50 ng/kg/day alfacalcidol orally as a daily dose by orogastric tube for 5 days before cisplatin injection. Then they received cisplatin in a dose and route similar to group II. Then they received the BM-MSCs suspension injected into the rat tail vein, in a dose of 2×10^6 in 0.5 ml PBS/rat one day after cisplatin injection. Then they continued alfacalcidol for another 5 days (Mazher et al., 2021; Abd Elsamie et al., 2023; LZ et al., 2013).

All rats from all groups were sacrificed by cervical dislocation on the 5th day of the experiment (Kelada et al., 2024).

Biochemical analysis

At the end of the experiment, venous blood (2 ml) was collected from retro-orbital venous plexus in dry clean non-heparinized test tubes. The samples were allowed to clot for 30-40 minutes at room temperature, then centrifugation was done at 2500 rpm for 15min. The serum was separated, and renal functions (blood urea nitrogen and serum creatinine) were evaluated using urea ELISA kit and creatinine ELISA kit. Abbot, Austria.

Histological assessment

Kidney tissues were obtained from euthanized rats for histological and immunohistochemical examination. The excised kidneys were cut into small specimens and fixed in 10% formol saline, processed by standard procedures and embedded in paraffin wax. Paraffin-embedded tissues were cut into 5 μ m thick sections.

The specimens were stained for examination of structural changes by Hematoxylin and eosin (H&E) stain, Masson's trichrome stain to demon-

strate collagen fibers and Periodic-Acid Schiff's (PAS) Stain. Sections were examined with an Olympus LM (Olympus BX41) equipped with spot digital camera (Olympus DP20) at CERMA (Cardiff et al., 2014; Feldman and Wolfe, 2014; Lau, 2019; Dey, 2018; Van et al., 2020).

Basement membrane thickness was assessed in PAS-stained sections by a blinded semi-quantitative scoring system. Five non-overlapping fields per rat (n=5 rats per group) were scored by two independent observers on a 0–3 scale: 0 = normal, 1 = mild thickening, 2 = moderate thickening, 3 = severe thickening. Mean \pm SD was calculated per group.

Immunohistochemical assessment

Immunohistochemical studies were applied to detect Rabbit Anti-active caspase-3 Monoclonal Antibody, Clone (EPR18297), Unconjugated (Abcam Cat# ab184787, Dilution: 1:1000) and Mouse Anti- TNF alpha Monoclonal Antibody (Elabscience Cat# E-AB-22159, Dilution: 1:50).

Active caspase-3 was selected as the apoptotic marker because it represents the principal executioner caspase downstream of both intrinsic and extrinsic pathways, mediating DNA fragmentation and cellular dismantling. It has been extensively validated as a sensitive and specific indicator of apoptosis in kidney tissue (DHO et al., 2025).

Paraffin-embedded kidney sections (4-5 μ m) were mounted on positively charged slides, deparaffinized in xylene, and rehydrated through descending grades of ethanol to distilled water. Antigen retrieval was carried out in citrate buffer (pH 6.0) at 95 °C for 15 min, and endogenous peroxidase activity was quenched with 3% hydrogen peroxide for 10 min. Non-specific binding was blocked using normal serum for 30 min at room temperature. Sections were then incubated overnight at 4 °C with Rabbit anti-active Caspase-3 monoclonal antibody (EPR18297) (Abcam, Cat# ab184787, 1:1000). After washing, slides were incubated with the appropriate biotinylated secondary antibody and streptavidin–HRP complex, using the Vectastain ABC-HRP kit (Vector Laboratories). Immunoreactivity was visualized with 3,3'-diaminobenzidine (DAB; Sigma) and coun-

terstained with Mayer's hematoxylin. Negative controls were processed by replacing the primary antibody with non-immune serum. Slides were dehydrated, mounted, and photographed with a Leica light microscope (Leica Microsystems, Switzerland)

Immunostained sections for caspase-3 and TNF- α were processed simultaneously to ensure identical exposure times to DAB. All slides were developed for exactly 3 minutes in DAB, rinsed in PBS, counterstained, and mounted together to minimize variability. Images were captured under the same illumination and camera settings. The brown DAB signal was quantified as the percentage of immunopositive area in five non-overlapping fields per section using Leica Qwin V.3 image analysis software. The mean percentage per animal was calculated and used for statistical comparison between groups (da Hora, et al., 2005; Cui et al., 2016; Mohamed and Shenouda et al., 2021),

For each marker (active caspase-3 and TNF- α), five non-overlapping cortical fields per section were randomly selected from five animals per group using a 40 \times objective. All images were captured under identical illumination and exposure settings to avoid bias. The area percentage of positive immunoreactivity (brown DAB staining) in the tubular epithelium and glomeruli was quantified using Leica QWin V3 image analysis software (Leica Microsystems, Wetzlar, Germany). The software threshold was calibrated once at the beginning of the analysis to detect only the positive DAB signal and applied uniformly across all groups. The mean area percentage of positive staining from all measured fields was calculated for each animal, and group means \pm SD were then derived. These data were used to compile Tables 5 and 6. Statistical comparisons between groups were performed as described in the Statistical Analysis section. (Varghese et al., 2014).

Morphometric analysis

The mean area percentage of collagen fibers stained with Masson's trichrome stain and the mean number of positive immune reactivity in the tubular epithelium were measured in five non-overlapping fields from five different sections of different rats in each group. Measurements

were performed at image analysis unit at the CERMA using Leica Q win V.3 program installed on a computer connected to a Leica DM2500 microscope (Wetzlar, Germany) (Abdelrahman et al., 2023; Mohamed and Shenouda et al., 2021).

Statistical analysis

All biochemical and morphometric results were analyzed using IBM SPSS software package version 20.0. (IBM Corp., Armonk, NY, USA). Kolmogorov-Smirnov test was used to verify the normality of distribution. Quantitative data were expressed as mean SD. ANOVA was used for normally distributed quantitative variables, to compare between more than two groups, and Post-Hoc test (Tukey), and were considered significant when $P \leq 0.05$ (Kotz et al., 2005; Kirkpatrick et al., 2015).

RESULTS

Morphology and Immunophenotype of BM-MSCs

Morphological Characterization by inverted phase contrast microscope

After a short period of cell culture, spindle adherent cells on the tissue culture plastic were formed. Proliferation of cells continued and confluence of 70-90% was reached within two weeks. Primary cells appeared adherent fusiform or polygonal in shape, having multiple small cytoplasmic projections. Cultures from passage 0 (P0), passage 1 (P1), passage 2 (P2) and passage 3 (P3) were photographed when they were almost semi-confluent (at 50%, 60%, 70%, 80% confluence respectively), denoting that cellular morphology and proliferative potential were maintained in the passages adopted in this study (Fig. 1a, b, c and d, respectively).

Characterization of BM-MSCs by Colony Forming Unit (CFU) assay

The CFU assay revealed that the cultured cells contained a subpopulation that can produce new fibroblast like colonies from single cells (Fig. 2).

Immunophenotyping of MSCs by flow cytometer

A flow cytometer analysis of the BM-MSCs from

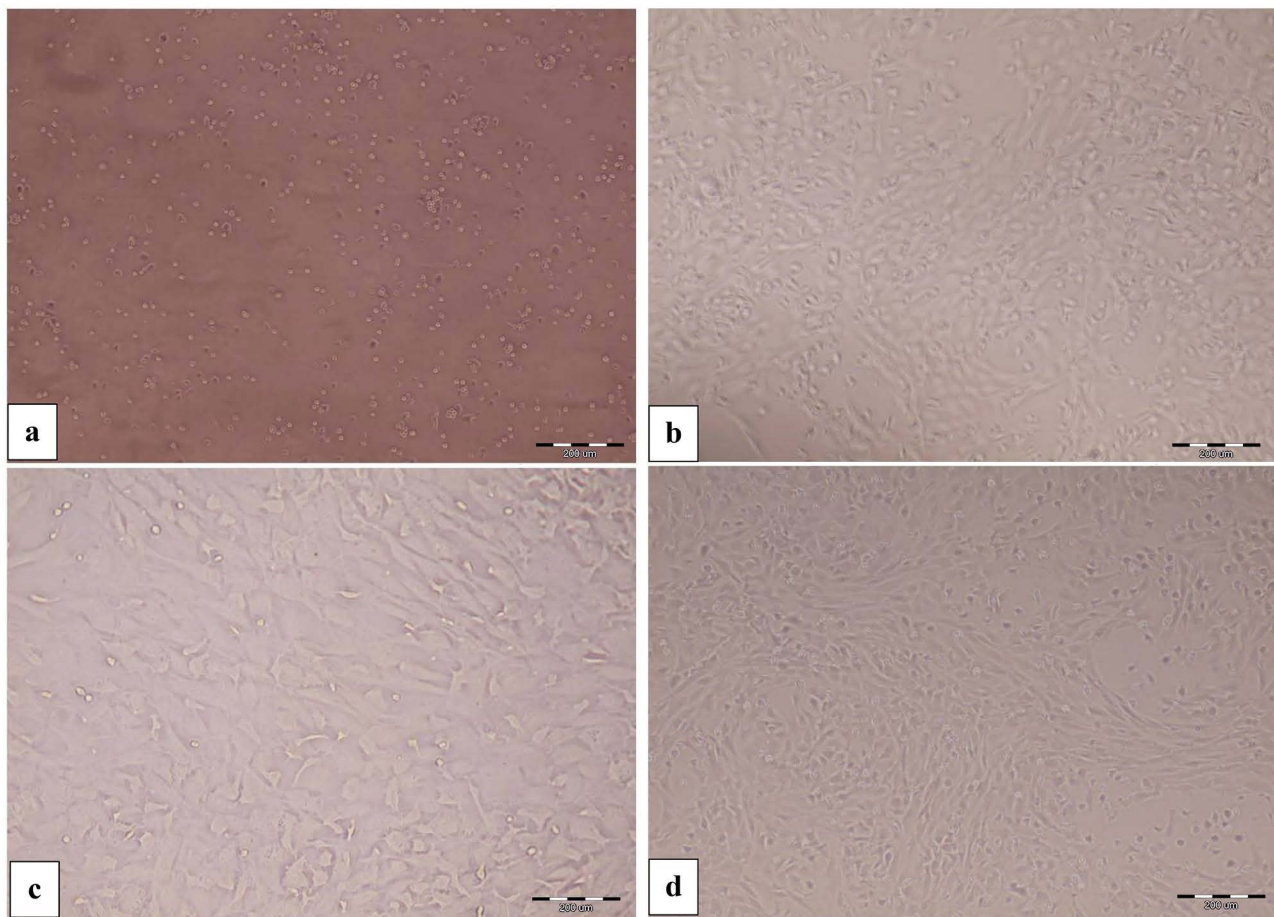


Fig. 1.- Morphological characterization of BM-MSCs showing large, flattened, spindle -shaped fibroblast -like cells. (a) P0 adherent fusiform cells with small cytoplasmic projections at 50% confluence. (b) P1 large spindle -shaped cells with 60% confluence. (c) P2 large spindle -shaped cells with 70% confluence. (d) P3 large spindle -shaped cells with 80% confluence. (Inverted phase contrast microscope, X 100). Scale bars: 200 µm.

P3 detected that they were positive for typical CD44 & CD90 surface markers. It demonstrated that 97.7 and 98.7% of the cultured BM-MSCs expressed CD44 and CD90 respectively. On the other hand, they were negative for the hematopoietic marker CD45 (Fig. 3 a-d).

Biochemical results

Statistical analysis of the collected data showed that there was a significantly high increase (P value < 0.001) in the blood urea nitrogen and serum creatinine levels in group II when compared to group I (control). On the other hand, treatment of cisplatin-induced nephrotoxicity with ALFA, BM-MSCs and their combination significantly reduced the serum creatinine and the blood urea level ($P < 0.05$) in comparison with the cisplatin group. There was an insignificant difference between groups IIIb and IIIc (Fig. 4a, b) (Tables 1 & 2).

Histological results

H & E stain results

H&E sections of the renal cortex of the Control group I showed normal renal corpuscles which appeared as spherical structures surrounded by Bowman's capsule enclosing a narrow urinary space. Proximal convoluted tubules (PCT) appeared having a narrow lumen and lined by a single layer of acidophilic cuboidal cells with evident apical brush border. The distal convoluted tubules (DCT) were having a wider lumen and lined by more cells at cross sections. Also, the cells lining the distal tubules were crowded at one side, forming the macula densa of the juxtaglomerular apparatus. The renal medulla showed the collecting ducts, lined with simple squamous to cuboidal epithelium with flattened to rounded vesicular nuclei, respectively (Fig. 5a, b).

Renal cortex of group II showed marked dis-

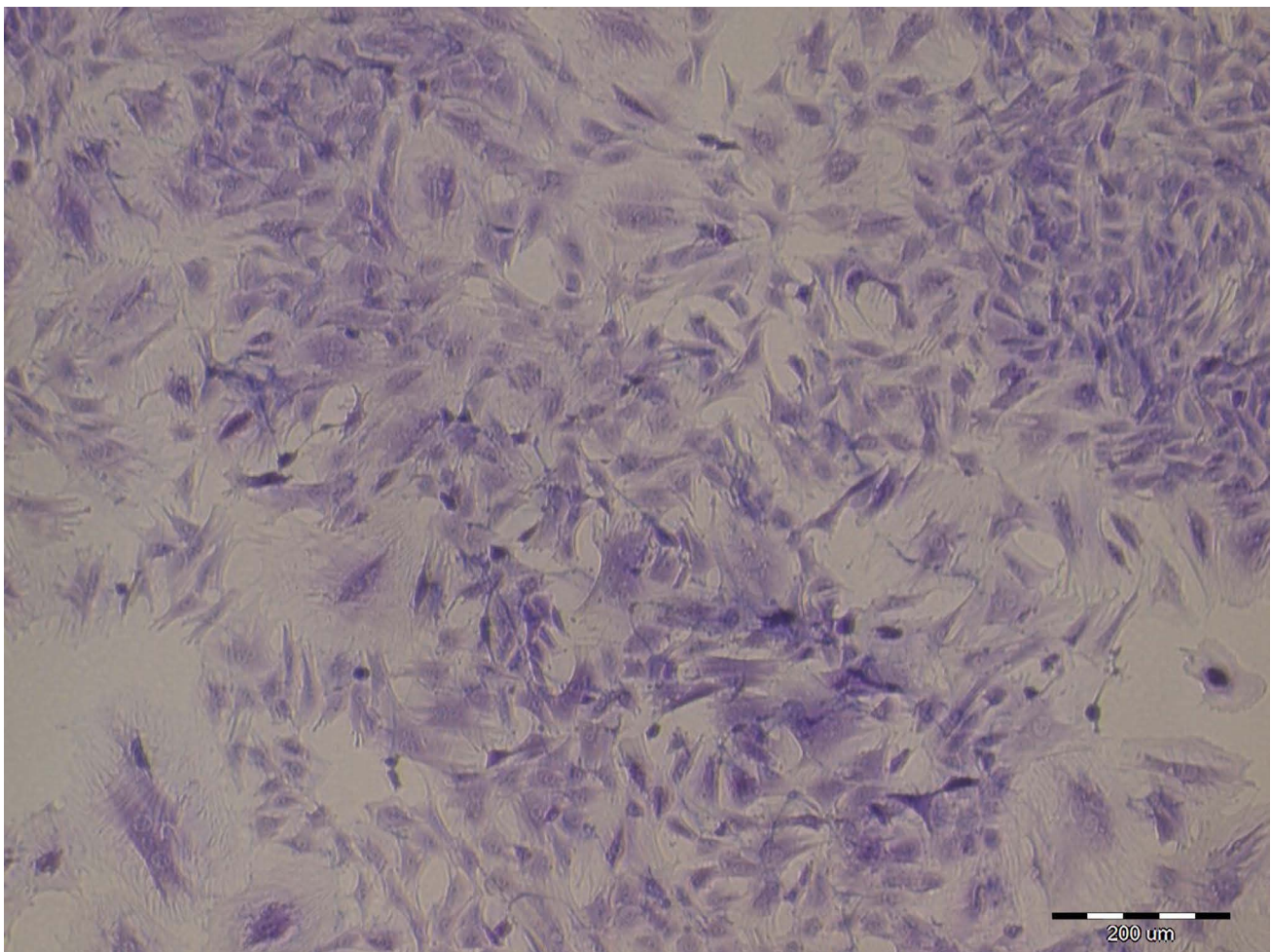


Fig. 2.- CFU assay for BM-MSCs at P3 using Crystal Violet stain showing several colonies. (Inverted phase contrast microscope, X 100). Scale bars: 200 μm .

ruption of the renal cortex histology, where some renal corpuscles appeared with a wide urinary space, and some appeared atrophied. Proximal and distal tubules appeared with widened lumina and were hardly distinguished. The tubular epithelium showed vacuolation, blebbing, desquamation into the lumina of the tubules. Moreover, homogeneous eosinophilic materials were detected in the lumina in some tubules. The epithelial cells lining some tubules showed pyknotic nuclei. Foci of inflammatory cells with flattened nuclei were noticed. Homogeneous acidophilic material (hyaline casts) was seen inside the lumen of some renal tubules. Moreover, there was marked congestion in the cortical blood vessels and in between the cortical tubules (Fig. 5 c-e).

Alfacalcidol-treated subgroup IIIa did not show any noticeable improvement, and most of the histopathological changes induced by cisplatin toxicity were still detected. These changes included the

distorted cortex with wide areas of degeneration, renal corpuscles with widened urinary space, and some corpuscles were atrophied. Proximal and distal tubules appeared with widened lumina with homogeneous eosinophilic materials. The tubular epithelium showed vacuolation, and some cells showed pyknotic nuclei. Inflammatory cells with flattened nuclei were noticed (Fig. 6a, b).

The BM-MSCs treated subgroup IIIb showed some improvement in the form of renal corpuscles with restored glomeruli, but still having wide urinary space. Some cells in the cortical tubules still showed cytoplasmic vacuolations, while the rest appeared with normal vesicular nuclei. The PCT regained their normal appearance; narrow lumen and apical brush border. Few inflammatory cells were seen (Fig. 6c, d).

BM-MSCs and-alfacalcidol-treated subgroup IIIc revealed obvious improvement with restoration of the renal corpuscles with intact glomeru-

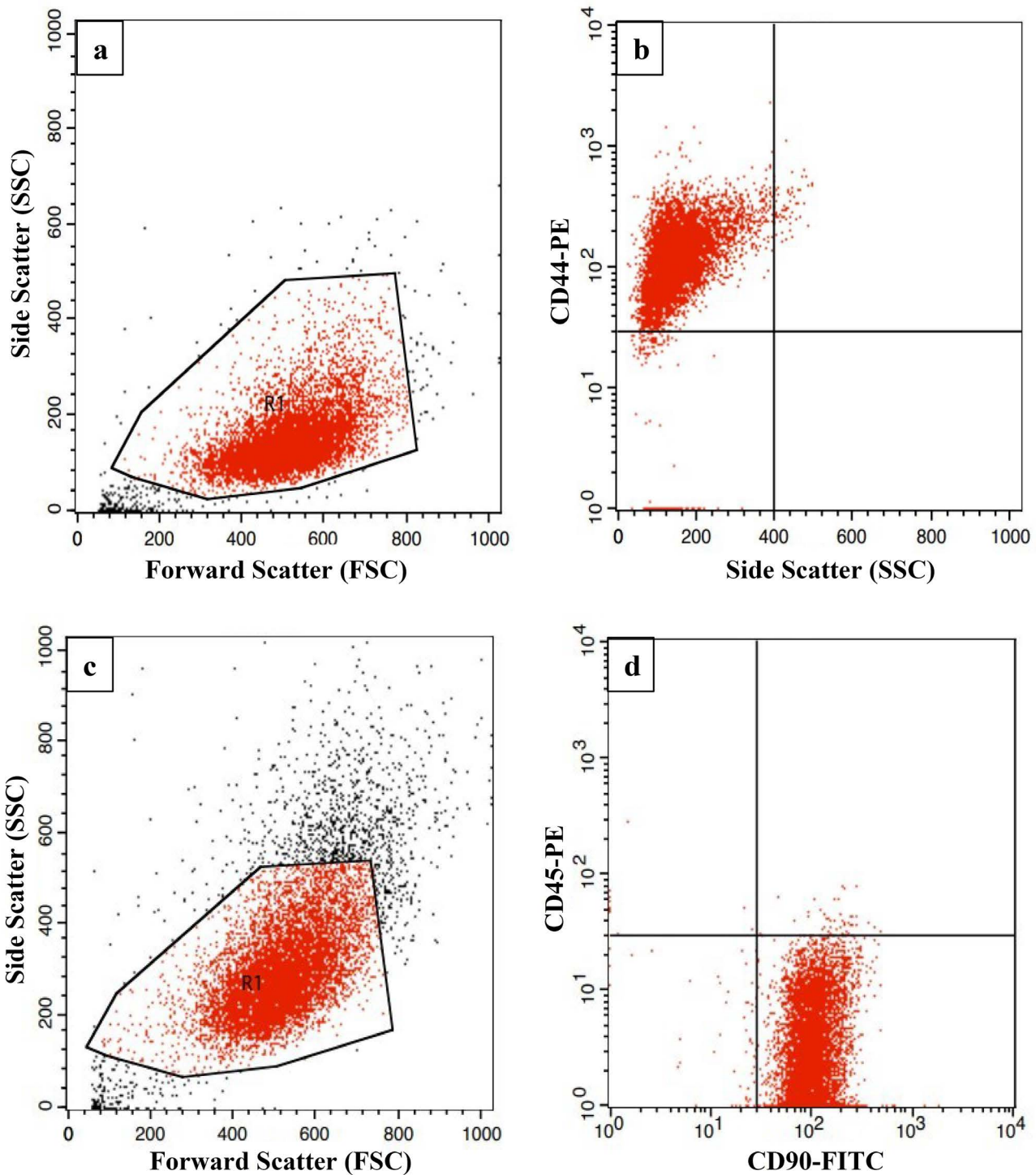


Fig. 3.- Flow cytometric analysis of cell-surface markers of BM-MSCs a, b: at P3, 97.74 % of the cultured cells expressed the mesenchymal cell marker CD44 in the upper left quadrant and c, d: at P3, 98.77% of the cultured cells expressed the mesenchymal cell marker CD90 in the lower right quadrant, while they were negative for the CD45 hematopoietic marker in the upper left quadrant.

li, Bowman’s capsule with ordinary urinary space, and most cells exhibited normal nuclei. The renal tubules restored their normal structure with apical brush border, and no inflammatory cells were observed (Fig. 6e, f).

Masson’s trichrome stain results

Masson’s trichrome stained sections revealed collagen deposition in the cortical interstitium around the renal corpuscles and the renal tubules. In the Control group I, the collagen deposition was

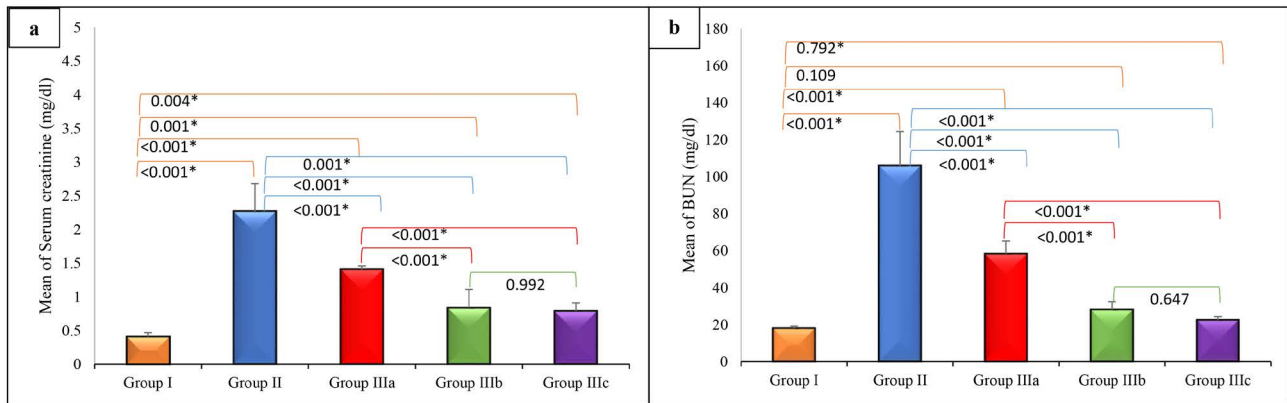


Fig. 4.- (a): Serum creatinine level (mg/dl) and (b): BUN level (mg/dl) in the studied groups.

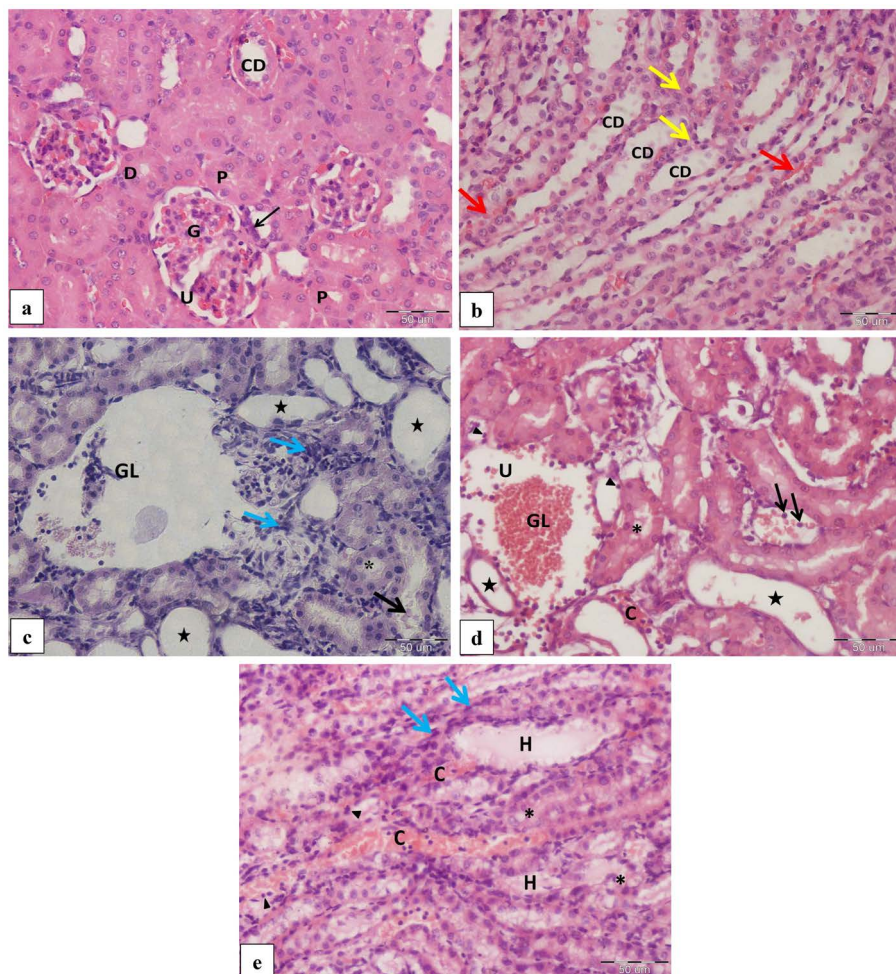


Fig. 5.- a: A photomicrograph of a section of rat's renal cortex of group I with normal renal architecture. The glomerulus (G) is surrounded by Bowman's capsule having an outer layer of simple squamous epithelium and an inner layer with podocytes and mesangial cells with a urinary space (U). The renal tubules are intact with preserved cytoplasm and nuclei. ↑ macula densa, (P) PCTs, (D) DCTs, (CD) collecting duct. b: A photomicrograph of a section of rat's renal medulla of group I showing the collecting ducts (CD), blood vessels between them (red arrow) and renal interstitium (yellow arrow). c-e: Photomicrographs of a section of group II showing: c: renal cortex of atrophied glomeruli (GL). Some tubules are dilated (black star) and no PCTs could be identified. Other tubules show cytoplasmic vacuolations and hydropic degeneration (*), while some tubules show desquamation of epithelial cells (black arrow). Inflammatory cells are seen (blue arrow). d: renal cortex showing destruction of the renal architecture. The glomeruli (GL) are atrophied with wide urinary space (U). Some tubules are dilated with flat epithelial lining (black star) and shedding of epithelial cells in the lumen (black arrow) and no PCTs could be identified. Some tubules show cells with pyknotic nuclei (arrowhead). Some cortical congested blood vessels (C) are seen. e: rat's renal medulla showing dilated renal tubules with acidophilic hyaline materials (H) in the lumen. Marked congestion and peritubular hemorrhage (C) are noticed. Some tubular cells show vacuolations (*) and others show pyknotic nuclei (arrowhead). Inflammatory cells (blue arrow) are seen. (H&E, X400). Scale bars: 50 µm.

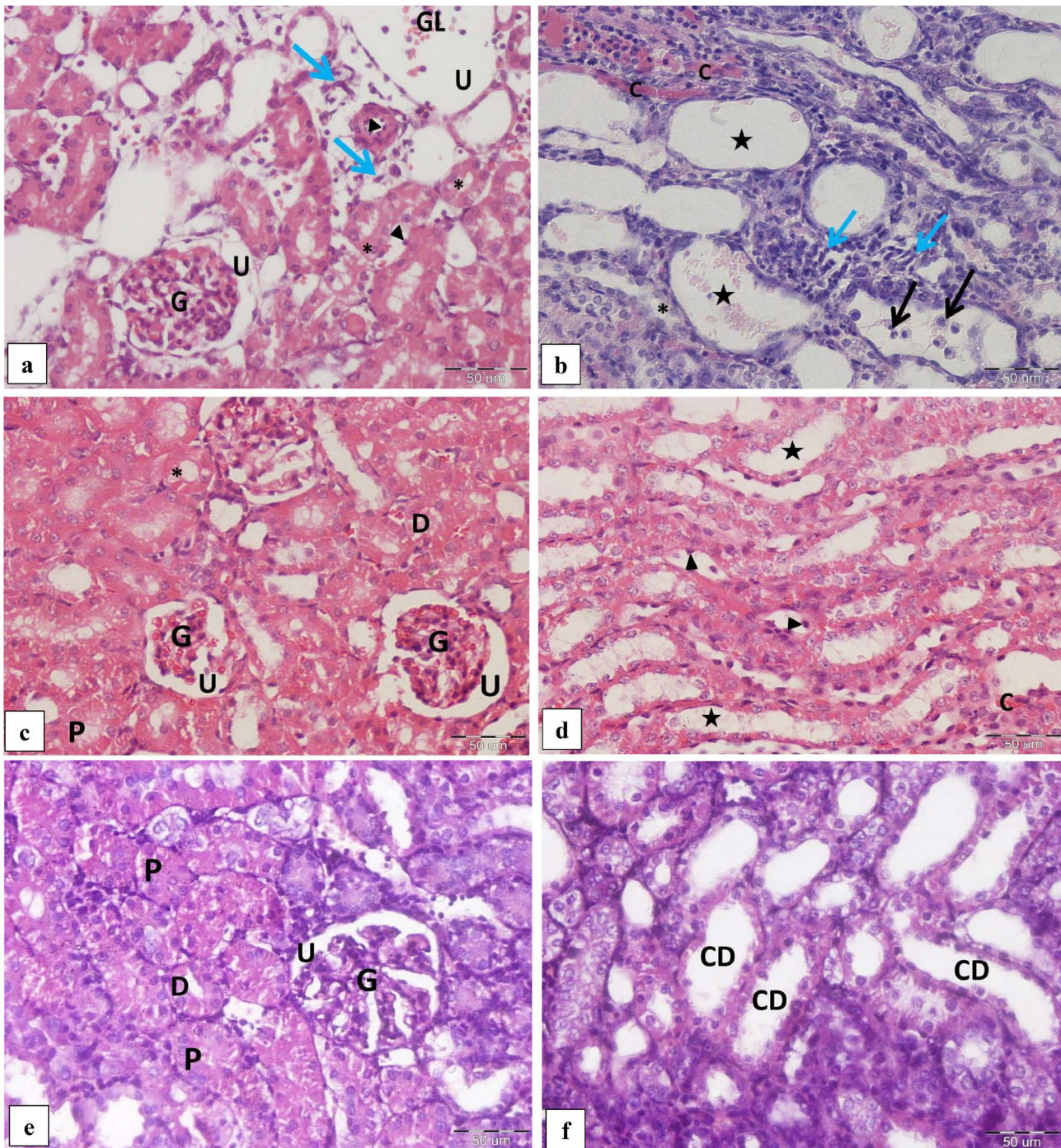


Fig. 6.- a & b: Photomicrographs of section of rat's kidney from group IIIa showing a: the cortex appearing with wide areas of degeneration and atrophied glomeruli (GL). Some glomeruli show wide urinary space (U). Some tubular cells show cytoplasmic vacuolations (*) and pyknotic nuclei (arrowheads). Large collections of inflammatory cells with flattened nuclei are seen (blue arrow). b: the medulla with dilatation of the renal tubules (black star). Some tubular cells show cytoplasmic vacuolations (*). Large collections of inflammatory cells with flattened nuclei are seen (blue arrow). Marked congestion and peritubular hemorrhage are seen in between the tubules (C). Some cells show sloughing of parts of their epithelium inside their lumina. c & d: Photomicrographs of section of rat's kidney from group IIIb showing c: the cortex appearing with nearly normal renal corpuscles with restored glomeruli (G) but still having wide urinary space (U). Few tubular cells show slight cytoplasmic vacuolations (v). Many normal PCTs (P) show regained apical brush borders, while few PCTs show loss of the apical brush border of the renal tubular epithelium (*). (D) DCT. d: the medulla appearing with dilatation of tubules (black star). Mild peritubular congestion is still seen (C). Some tubular cells show pyknotic nuclei (arrowhead). e & f: Photomicrographs of a section of rat's kidney from group IIIc showing e: restoration of the renal corpuscles with intact glomeruli (G), layers of Bowman's capsule with ordinary urinary space (U). Most cells exhibit normal nuclei, and the tubules restored their normal structure. PCTs (P) show apical brush border. No inflammatory cells are observed. (D) DCT. f: renal medullary tubules of regular structure lined with simple cuboidal cells featuring rounded vesicular nuclei and acidophilic cytoplasm. No inflammatory cells are observed. (CD) Collecting duct. (H&E stain, X400). Scale bars: 50 μ m.

Table 1. Serum creatinine level (mg/dl) in the studied groups

Biochemical	Group I (n = 10)	Group II (n = 10)	Group IIIa (n = 10)	Group IIIb (n = 10)	Group IIIc (n = 10)	F	P
Serum creatinine (mg/dl) Min. – Max.	0.32 – 0.48	1.65 – 2.80	1.35 – 1.52	0.56 – 1.20	0.60 – 0.97	100.802*	<0.001*
Mean ± SD	0.41 ± 0.06	2.27 ± 0.41	1.41 ± 0.05	0.84 ± 0.27	0.79 ± 0.12		
p1		<0.001*	<0.001*	0.001*	0.004*		
p2			<0.001*	<0.001*	<0.001*		
p3				<0.001*	<0.001*		
p4					0.992		

SD: Standard deviation F: F for One way ANOVA test, Pairwise comparison between each 2 groups was done using Post Hoc Test (Tukey)

p: p value for comparing the studied groups

p1: p value for comparing Group I and each other groups

p2: p value for comparing Group II and each other groups

p3: p value for comparing Group IIIa and each other groups

p4: p value for comparing Group IIIb and Group IIIc

*: Statistically significant at $p \leq 0.05$

Group I: Control

Group II: Cisplatin

Group IIIa: ALFA-treated group

Group IIIb: Stem cell-treated

Group IIIc: ALFA+ stem cell-treated

Table 2. BUN level (mg/dl) in the studied groups

Biochemical	Group I (n = 10)	Group II (n = 10)	Group IIIa (n = 10)	Group IIIb (n = 10)	Group IIIc (n = 10)	F	P
BUN (mg/dl) Min. – Max.	16.40 – 19.60	78.0 – 130.0	49.0 – 70.0	22.40 – 35.0	21.0 – 26.0	165.905*	<0.001*
Mean ± SD	18.06 ± 1.13	106.0 ± 18.35	58.40 ± 6.88	28.14 ± 4.27	22.60 ± 1.78		
p1		<0.001*	<0.001*	0.109	0.792		
p2			<0.001*	<0.001*	<0.001*		
p3				<0.001*	<0.001*		
p4					0.647		

SD: Standard deviation

F: F for One way ANOVA test, Pairwise comparison between each 2 groups was done using Post Hoc Test (Tukey)

p: p value for comparing the studied groups

p1: p value for comparing Group I and each other groups

p2: p value for comparing Group II and each other groups

p3: p value for comparing Group IIIa and each other groups

p4: p value for comparing Group IIIb and Group IIIc

*: Statistically significant at $p \leq 0.05$

Group I: Control

Group II: Cisplatin

Group IIIa: ALFA-treated group

Group IIIb: Stem cell-treated

Group IIIc: ALFA+ stem cell-treated

minimal and appeared as a thin rim surrounding the cortical structures.

However, in group II and the Alfacalcidol-treated subgroup IIIa, collagen deposition was evident and markedly increased in comparison to the control group. While, in BM-MSCs-treated subgroup IIIb, collagen deposition was noticeably decreased. The BM-MSCs-and-alfacalcidol-treated

subgroup IIIc almost revealed no apparent difference in collagen deposition from the control group (Fig. 7 a-e). These findings were further morphologically measured and statistically analyzed to confirm the microscopic results (Table 3).

PAS stain results

Sections of the Control group I showed PAS positive reaction in the basement membranes of pa-

Table 3. Mean percentage of fibrosis in the studied groups

	Group I (n = 10)	Group II (n = 10)	Group IIIa (n = 10)	Group IIIb (n = 10)	Group IIIc (n = 10)	F	P
Percentage of fibrosis							
Min. – Max.	8.96 – 10.77	34.46 – 47.08	14.91 – 19.30	10.05 – 14.63	10.89 – 12.62	279.974*	<0.001*
Mean ± SD	9.86 ± 0.57	38.95 ± 4.50	17.34 ± 1.68	12.38 ± 1.42	11.57 ± 0.61		
p1		<0.001*	<0.001*	0.115	0.458		
p2			<0.001*	<0.001*	<0.001*		
p3				<0.001*	<0.001*		
p4					0.931		

SD: Standard deviation

F: F for One way ANOVA test, Pairwise comparison between each 2 groups was done using Post Hoc Test (Tukey)

p: p value for comparing the studied groups

p1: p value for comparing Group I and each other groups

p2: p value for comparing Group II and each other groups

p3: p value for comparing Group IIIa and each other groups

p4: p value for comparing Group IIIb and Group IIIc

*: Statistically significant at $p \leq 0.05$

Group I: Control

Group II: Cisplatin

Group IIIa: ALFA-treated group

Group IIIb: Stem cell-treated

Group IIIc: ALFA+ stem cell-treated

Group IIIc: ALFA+ stem cell-treated

Table 4. Semi-quantitative scoring of basement membrane thickness in PAS-stained sections

Group	Score 0 (Normal)	Score 1 (Mild)	Score 2 (Moderate)	Score 3 (Severe)	Mean ± SD
Group I (Control)	25	0	0	0	0.00 ± 0.00
Group II (Cisplatin)	0	3	8	14	2.44 ± 0.51
Group IIIa (Alfacalcidol)	4	9	10	2	1.56 ± 0.63
Group IIIb (BM-MSCs)	9	11	5	0	1.00 ± 0.45
Group IIIc (BM-MSCs + Alfacalcidol)	15	8	2	0	0.56 ± 0.38

Values indicate number of fields scored in each category (five fields × five rats = 25 fields per group).

rietal layer of Bowman's capsule and of convoluted tubules, as well as brush borders of proximal tubules.

The cortex of group II and the Alfacalcidol-treated subgroup IIIa showed renal corpuscles with noticeably widened tubules. It revealed focal loss of PAS reaction in most of the PCT, complete or partial loss of their brush borders with thickened basement membrane.

In BM-MSCs-treated subgroup IIIb, the cortex showed some PCT with restored brush border, while some PCT still showed loss of their brush border. Thickening of the basement membrane was still noticed. The BM-MSCs-and-alfacalcidol-treated subgroup IIIc revealed that PAS positive reaction was more or less similar to the control group (Fig. 8 a-e).

Basement membrane thickness was evaluated in PAS-stained sections, using a blinded semi-quantitative scoring system. Group II (cisplatin) showed the highest scores indicating severe thickening, whereas Groups IIIb and IIIc showed markedly reduced scores approaching control values (Table 4).

Immunohistochemical results

Detection of active caspase-3 in apoptotic cells: (Table 4)

The control group (group I) showed very weak cytoplasmic caspase-3 reaction in the glomeruli of renal corpuscle, as well as cells lining renal tubules in comparison to Cisplatin group (group II), which showed intense positive cytoplasmic re-

Table 5. Percentage of active caspase-3 immunostaining in the studied groups

	Group I (n = 10)	Group II (n = 10)	Group IIIa (n = 10)	Group IIIb (n = 10)	Group IIIc (n = 10)	F	P
Area % of active caspase 3 Min. – Max.	2.84 – 7.10	54.68 – 63.76	37.49 – 44.34	25.84 – 30.82	15.57 – 20.07	948.064*	<0.001*
Mean ± SD	4.76 ± 1.60	59.29 ± 3.19	40.32 ± 2.16	28.36 ± 1.79	17.88 ± 1.58		
p1		<0.001*	<0.001*	<0.001*	<0.001*		
p2			<0.001*	<0.001*	<0.001*		
p3				<0.001*	<0.001*		
p4					<0.001*		

SD: Standard deviation

F: F for One way ANOVA test, Pairwise comparison between each 2 groups was done using Post Hoc Test (Tukey)

p: p value for comparing the studied groups

p1: p value for comparing Group I and each other groups

p2: p value for comparing Group II and each other groups

p3: p value for comparing Group IIIa and each other groups

p4: p value for comparing Group IIIb and Group IIIc

*: Statistically significant at $p \leq 0.05$

Group I: Control

Group II: Cisplatin

Group IIIa: ALFA-treated group

Group IIIb: Stem cell-treated

Group IIIc: ALFA+ stem cell-treated

action with significant difference ($P \leq 0.05$) from control group (Table 5).

The alfacalcidol-treated group (group IIIa) showed high positive cytoplasmic caspase-3 reaction in the glomeruli, together with nuclear and cytoplasmic expression in the renal lining tubular cells with a significant difference ($P \leq 0.05$) from control group as well as cisplatin group (Table 5).

The MSCs- treated group (group IIIb) showed moderate positive cytoplasmic expression of caspase-3 in the glomeruli, as well as cytoplasmic and nuclear reaction in some renal tubular cells, with a significant difference ($P \leq 0.05$) from the control group, cisplatin group, as well as alfacalcidol-treated group (Table 5).

The combined Alfacalcidol-and-MSCs-treated group (group IIIc) showed few positive cytoplasmic reactions of caspase-3 in the glomeruli with cytoplasmic and nuclear expression in the renal tubular cells, with a significant difference ($P \leq 0.05$) from control group, cisplatin group, alfacalcidol treated group and MSCs – treated group (Fig. 9 a-f).

Detection of tumor necrosis factor α (TNF- α) in renal tissue

Control group (group I) showed very weak cytoplasmic TNF- α reaction in the glomeruli of renal corpuscle as well as cells lining renal tubules.

Cisplatin group (group II) showed intense positive cytoplasmic TNF- α reaction along glomerulus, as well as cytoplasmic and nuclear reaction of cells lining renal tubules with a significant difference ($P \leq 0.05$) from control group (Table 6).

Alfacalcidol- treated group (group IIIa) showed high positive cytoplasmic TNF- α reaction in the glomeruli, together with nuclear and cytoplasmic expression in cells lining renal tubules, with a significant difference ($P \leq 0.05$) from control group as well as cisplatin group (Table 6).

MSCs- treated group (group IIIb) showed moderate positive cytoplasmic expression of TNF- α in the glomeruli, as well as cytoplasmic and nuclear reaction cells lining some renal tubules, with a significant difference ($P \leq 0.05$) from control group, cisplatin group, as well as alfacalcidol treated group.

Alfacalcidol-and-MSCs-treated group (group IIIc) showed weak positive cytoplasmic reaction of TNF- α in the glomeruli, together with weak cytoplasmic and nuclear reaction in the renal tubular cells, with a significant difference ($P \leq 0.05$) from

Table 6. Percentage of TNF- α immunostaining in the studied groups

	Group I (n = 10)	Group II (n = 10)	Group IIIa (n = 10)	Group IIIb (n = 10)	Group IIIc (n = 10)	F	P
Area % of TNF- Min. – Max.	1.23 – 3.57	53.02 – 64.24	40.03 – 47.83	32.70 – 39.51	17.89 – 22.70	842.916*	<0.001*
Mean \pm SD	2.53 \pm 0.79	59.86 \pm 3.82	43.86 \pm 2.54	35.33 \pm 2.22	19.87 \pm 1.50		
p1		<0.001*	<0.001*	<0.001*	<0.001*		
p2			<0.001*	<0.001*	<0.001*		
p3				<0.001*	<0.001*		
p4					<0.001*		

SD: Standard deviation

F: F for One way ANOVA test, Pairwise comparison between each 2 groups was done using Post Hoc Test (Tukey)

p: p value for comparing the studied groups

p1: p value for comparing Group I and each other groups

p2: p value for comparing Group II and each other groups

p3: p value for comparing Group IIIa and each other groups

p4: p value for comparing Group IIIb and Group IIIc

*: Statistically significant at $p \leq 0.05$

Group I: Control

Group II: Cisplatin

Group IIIa: ALFA-treated group

Group IIIb: Stem cell-treated

Group IIIc: ALFA+ stem cell-treated

control group, cisplatin group, alfacalcidol-treated group and MSCs – treated group (Fig. 10 a-f) (Table 6).

Morphometric results

Sections stained by Masson's trichrome showed that the mean area percentage of collagen fibers deposition in the renal cortex in cisplatin group (group II) was increased significantly in comparison with control group (group I). Treatment of cisplatin-induced acute nephrotoxicity with alfacalcidol (group IIIa), MSCs (group IIIb), and their combination (group IIIc) significantly reduced the percentage of fibrosis ($P \leq 0.05$) in comparison with the cisplatin group (group II). No significant difference was shown between the MSCs (group IIIb) and the combined-treated groups (group IIIc) (Table 3).

The mean area percentage of caspase-3 immunostaining in the renal cortex showed a significant increase in the cisplatin group (group II) in comparison with the control (group I) and other treated groups. A significant decrease in caspase-3 immunoexpression in the MSCs-treated group (group IIIb) was observed in comparison with alfacalcidol-treated (group IIIa). Moreover,

caspase-3 immunoexpression was significantly decreased in the combined treated group (group IIIc) in comparison to group IIIa and group IIIb (Table 5).

The mean area percentage of TNF- α immunostaining in the renal cortex was highly increased in the cisplatin group (group II) in comparison to the control (group I) and other treated groups. A significant decrease in the TNF- α immunoexpression in the MSCs-treated group (group IIIb) was observed in comparison to alfacalcidol-treated (group IIIa). Moreover, TNF- α immunoexpression was significantly decreased in the combined treated group (group IIIc) in comparison to group IIIa and group IIIb (Table 5).

DISCUSSION

Although vitamin-D analogues and MSCs have each demonstrated renoprotective effects in acute kidney injury, their combined use in cisplatin-induced nephrotoxicity has not yet been explored. We hypothesized that alfacalcidol would complement the effects of MSCs, providing greater protection of renal structure and function.

The destructive effects of cisplatin were shown in the current study, such as altered architecture

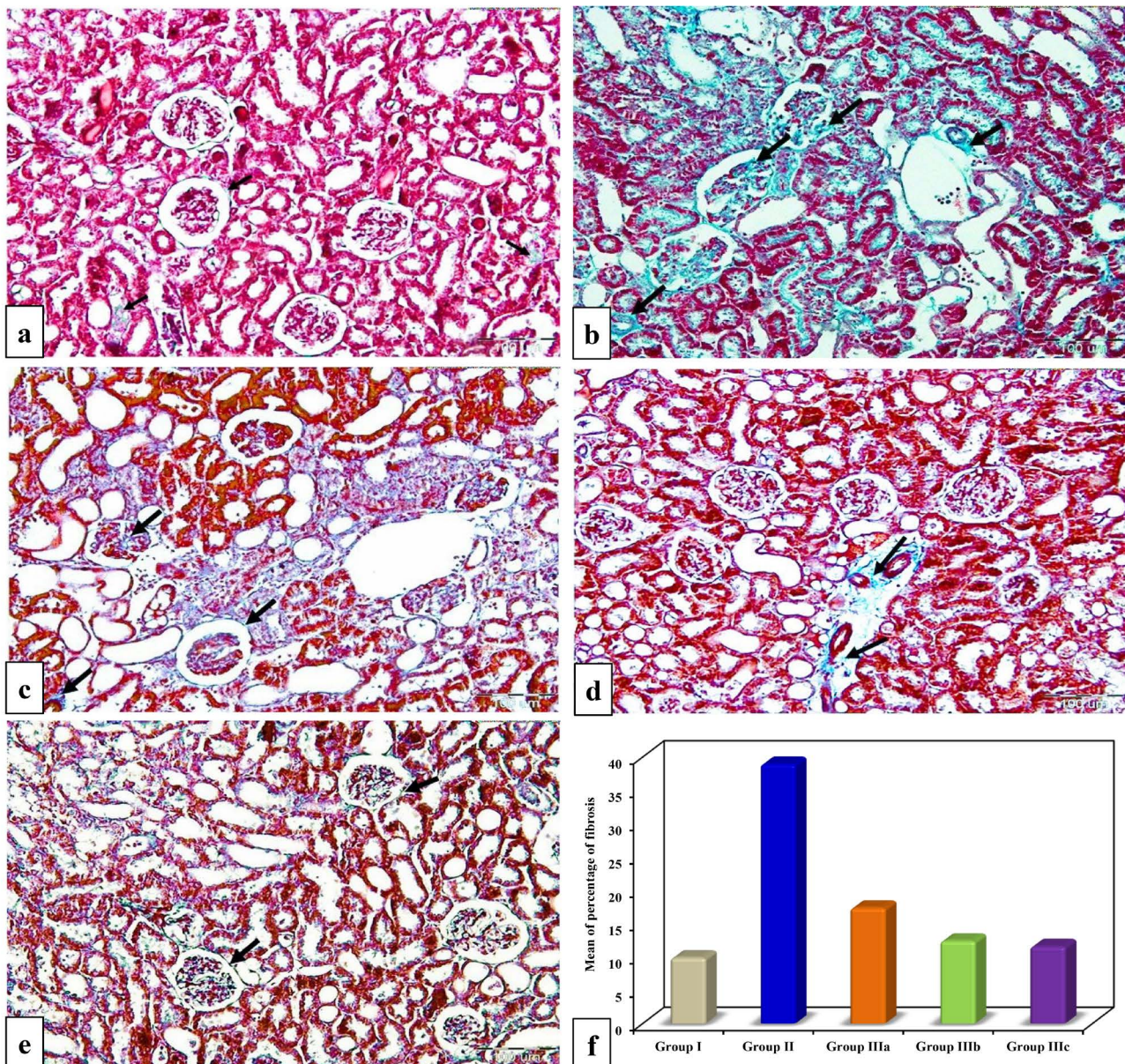


Fig. 7.- (a-f): A photomicrograph of a section of rat's kidney of (a): group I showing minimal deposition of collagen fibers (blue color) in the renal corpuscles and renal tubules (black arrows), (b): group II showing intense deposition of collagen fibers in the renal corpuscles together with interstitial fibrosis (black arrows), (c): group IIIa showing deposition of collagen fibers in the renal corpuscles and interstitial tissue (black arrows), (d): group IIIb showing deposition of collagen fibers mainly in the interstitial tissues (black arrows), (e): group IIIc showing mild deposition of collagen fibers in the renal corpuscles and interstitial tissue (black arrows) (Masson's trichrome, X200) Scale bars: 100 μ m. (f): Mean percentage of fibrosis in the studied groups.

of the kidney, degenerative changes of the renal corpuscles with atrophy of the glomeruli and widened urinary spaces. Also, the renal tubules were dilated, having cytoplasmic vacuolization, pyknotic nuclei, desquamated epithelial cells and intraluminal cast formation with loss of the characteristic brush border of PCTs. Moreover, there were interstitial inflammatory cellular infiltration and vascular congestion. Similar findings were mentioned in other studies (Ghaly et al., 2014, Boulikas et al., 2003).

The actual mechanism of cisplatin-induced nephrotoxicity is still unknown, and different theories were reported. Among these mechanisms are DNA damage, mitochondrial dysfunction, lipid peroxidation, and structural protein degradation (Saad et al., 2009; Basnakian et al., 2005; Ali and Al Moundhri, 2006).

Many authors proved that the direct tubular damage caused by cisplatin is due to binding of its platinum component to DNA with formation of in-

ter- and intra-strand cross-links, thereby halting DNA synthesis and replication inducing molecular damage with consequent apoptosis. Moreover, cisplatin-induced mitochondrial dysfunction led to DNA damage, with increased production of ROS and free radicals and oxidative stress (Ghaly et al., 2014; Qi et al., 2013). This is consistent with in-

creased caspase-3 immunoreactivity in cisplatin group in the current study, and with the results of other studies (Abdelrahman et al., 2023; Abd Elsamie et al., 2023; LZ et al., 2013; Ramesh and Reeves, 2003).

The cisplatin apoptotic pathways include the intrinsic pathway involving the cell organelles

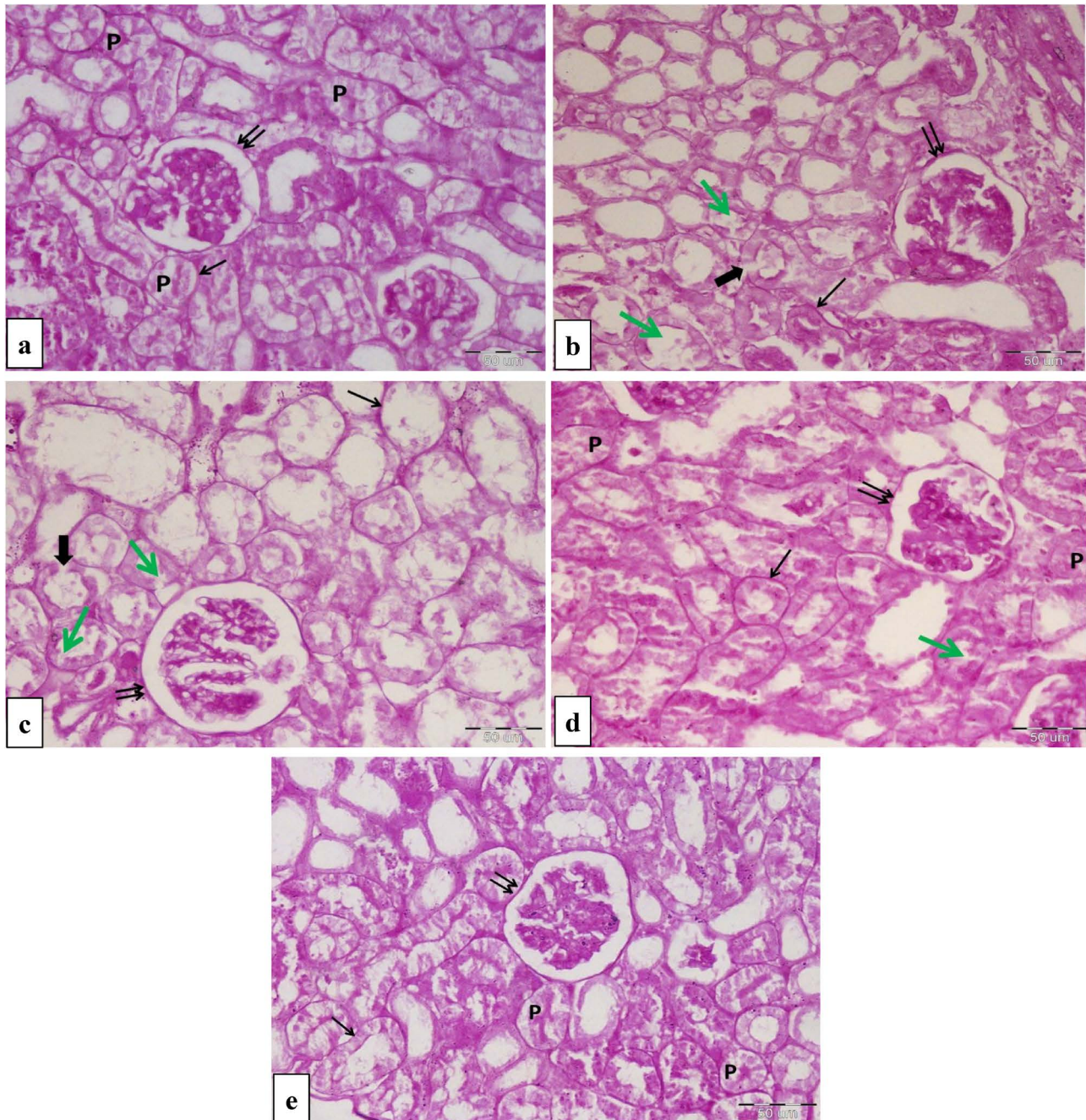


Fig. 8.- (a-e): A photomicrograph of a section of rat's kidney of (a): group I showing a strong positive reaction (dense magenta red color) in the brush border of the PCTs (P) as well as the glomerular (2 arrows) and tubular (thin arrow) basement membranes, (b): group II demonstrates complete or partial loss of the brush border (green arrow) in most of the PCTs. Some renal tubules show disruption of their basement membranes (thick arrow) while other tubules show thickening of the basement membrane (thin arrow). Thickening of the GBM (2 arrows) could be seen, (c): group IIIa showing partial or complete loss of the brush border of the PCTs (green arrow). Some renal tubules show disruption of their basement membrane (thick arrow) while others demonstrate thickened basement membrane (thin arrow). Thickening of the GBM (2 arrows) could be seen, (d): group IIIb showing some PCTs that restored their brush border (P) while other tubules still show loss of apical brush border (green arrow). Thickening of the basement membrane of some tubules (thin arrow) together with slight thickening of the GBM (2 arrows) is observed, (e): group IIIc showing more or less normal thickening of the glomerular (2 arrows) and tubular (thin arrow) basement membranes. Most of the PCTs restored their brush borders (P). (PAS, X400). Scale bars: 50 µm.

like mitochondria and endoplasmic reticulum, together with the extrinsic pathway, also known as the death receptor pathway, which involves the activation of death receptors in response to binding membrane receptors. These pathways lead to

the activation of specific proteases called executioner caspases, including caspase-3 (Peres and Cunha, 2013).

Desquamation of the renal tubular epithelial cells caused by cisplatin in the current study may

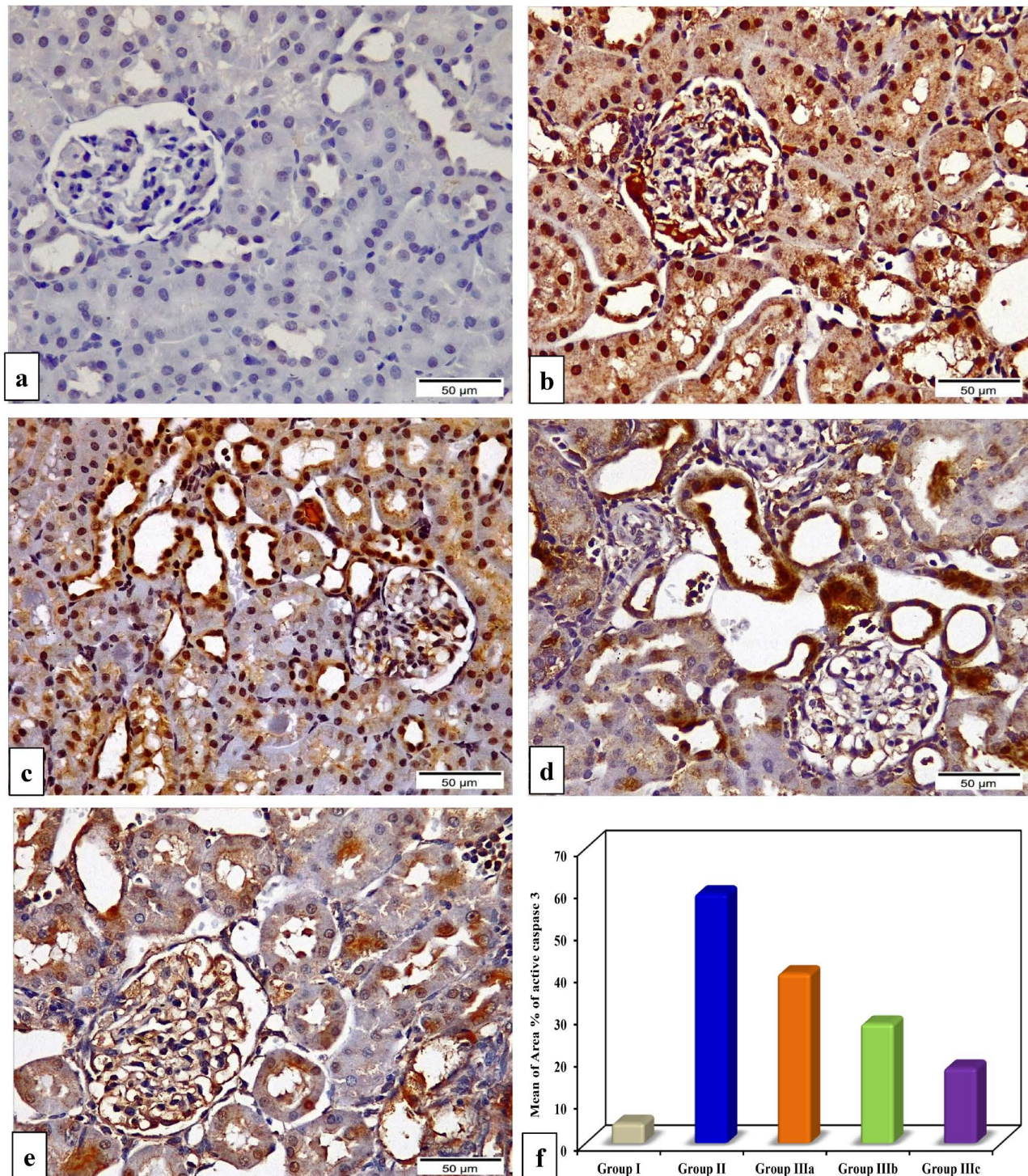


Fig. 9.- (a-f): A photomicrograph of a section of rat's kidney of (a): group I showing scarce cytoplasmic caspase-3 reaction along the renal corpuscles as well as renal tubules, (b): group II showing intense positive cytoplasmic caspase-3 reaction along the renal glomeruli as well as cytoplasmic and nuclear reactions in the cells lining renal tubules, (c): group IIIa showing a positive cytoplasmic caspase-3 reaction along the glomeruli together with nuclear and cytoplasmic expression along cells lining renal tubules, (d): group IIIb showing a moderate positive cytoplasmic expression of caspase-3 along the renal glomeruli as well as cytoplasmic and nuclear reaction along some renal tubular cells, (e): group IIIc showing low positive cytoplasmic reaction of caspase-3 along the renal glomeruli and few cytoplasmic and nuclear reactivity to cells lining renal tubules. (Caspase-3 immunostaining X 400) (f): Percentage of active caspase-3 immunostaining in the studied groups. Scale bars: 50 µm.

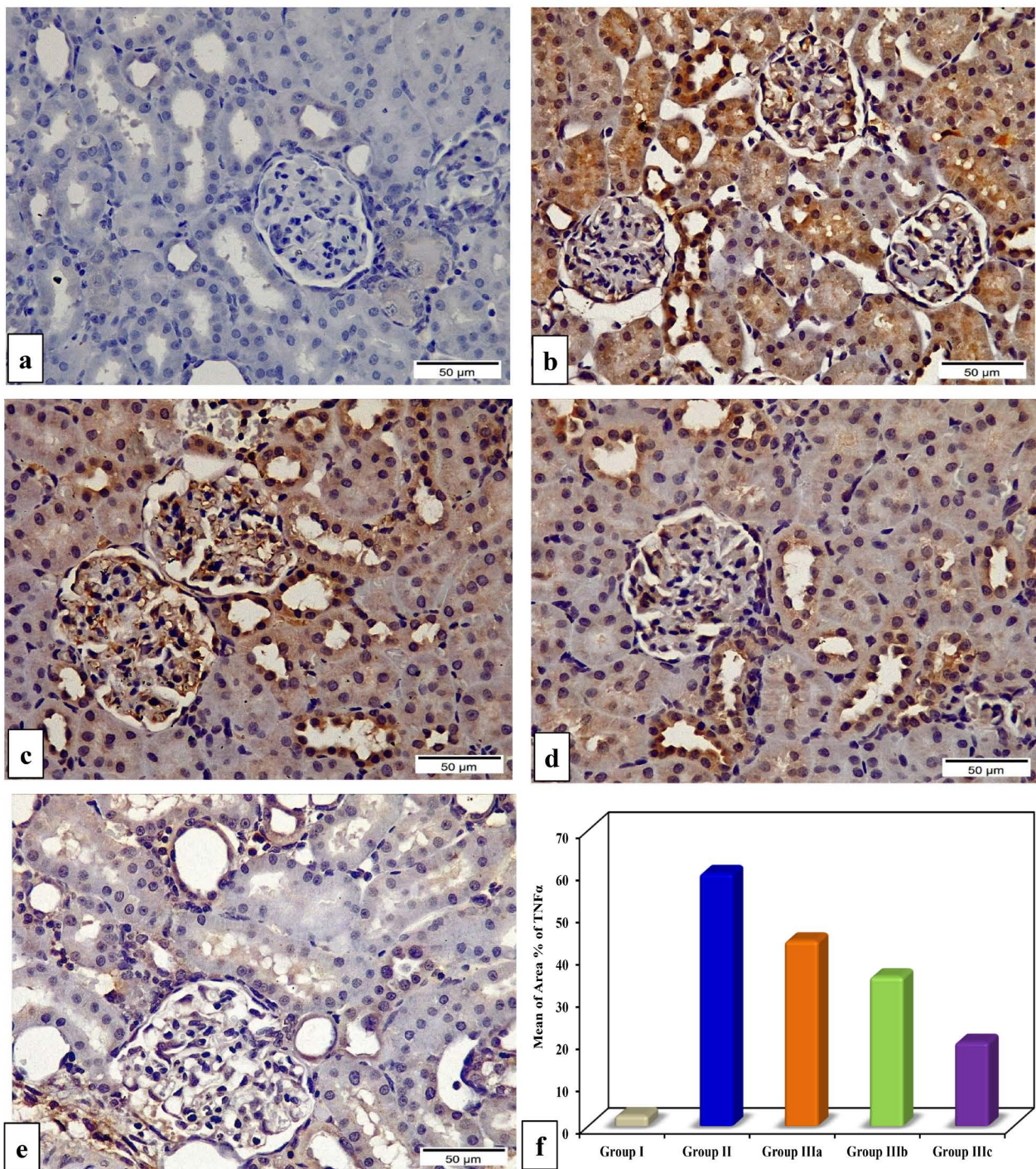


Fig. 10.- (a-f): A photomicrograph of a section of rat’s kidney of (a): group I showing scarce cytoplasmic TNF- α reaction along the renal glomeruli as well as the renal tubular cell, (b): group II showing a strong positive cytoplasmic TNF- α reaction along the renal glomeruli with cytoplasmic and nuclear reaction in the renal tubular lining cells, (c): group IIIa showing a positive cytoplasmic TNF- α expression along the glomeruli together with cytoplasm and nuclei of some cells lining the renal tubule. (d): group IIIb showing moderate positive cytoplasmic expression of TNF- α along the glomeruli as well as the cytoplasm and nuclei of some renal tubular lining cells. (e): group IIIc showing low positive cytoplasmic reactions of TNF- α along the glomeruli and cells lining the renal tubules. (TNF- α immunostaining X 400). (f): Percentage of TNF- α immunostaining in the studied groups. Scale bars: 50 μ m.

be explained by redistribution or alteration of integrin, which anchors the tubular cells (Abd El Zaher et al., 2017; Kumar et al., 2013). The interaction of the detached tubular epithelial cells and their debris with tubular lumen proteins results

in the development of intraluminal hyaline casts (Sadek et al., 2016). This may cause obstruction of urine flow and elevation of intra-tubular pressure, with tubular dilatation and flattening of tubular cells. This aggravated by intrarenal vasoconstrictic-

tion linked to AKI, with subsequent cellular atrophy (Kumar et al., 2013).

It was discovered that absorption of cisplatin occurs primarily in the PCTs, followed by the DCTs, so that the concentration of cisplatin in PCTs is approximately five times higher than that in the plasma (Abdelrahman et al., 2023; Kodama et al., 2014).

The current study demonstrated marked affection of PCTs with loss of their characteristic brush border proved by weak PAS reaction. This is considered a key sign of kidney damage that was also proved by other studies (Abd El Zaher et al., 2017; Abdelrahman et al., 2023; Kelada et al., 2024). This can be explained by the production of ROS, resulting in loss of brush border microvilli and cell junctions. Additionally, adhesion molecules and other membrane proteins and integrins, are mis localized (Bonventre et al., 2011).

The significant thickening of the glomerular and tubular basement membrane caused by cisplatin in the current study was also mentioned by Abdelrahman et al. 2023, Ghaly et al., 2014 and Mazher et al., 2021. This might result from accumulation of glycoproteins as a result of renal injury and the upregulation of integrin, laminin, and fibronectin (Ghaly et al., 2014; Chen and Tuan, 2008).

The interstitial inflammatory cellular infiltration and high expression of TNF- α caused by cisplatin in the current study are indicative of inflammation. These findings were consistent with those of Abdelrahman et al. (2023), Abd Elsamie et al. (2023), Ramesh et al. (2003) and Kelada et al. (2024). The dead tubular cells could recruit inflammatory cells, together with increased expression of many inflammatory chemokines and cytokines, including IL-1 α and TNF- α (Chang et al., 2002). Also, cisplatin promotes the transcription of genes encoding inflammatory mediators. Moreover, the dilatation of peritubular capillaries and extravasation of RBCs seen in the cisplatin group may be related to renal endothelial cell death and renal dysfunction (Qi and Wu, 2013, Abd Elsamie et al., 2023; Peres and Cunha, 2013; Elseweidy et al., 2018).

In the current study, fibrotic changes, whether glomerular, tubular or interstitial, were observed

in the cisplatin group and this was also reported by Zahran et al. (2016).

It was stated that macrophages might contribute significantly to the renal interstitial fibrosis through the production of certain fibrogenic factors such as TNF- α and TGF- α . These factors promote the generation of myofibroblasts, which lay down extracellular matrix (Curtis et al., 2008). Moreover, activated and phenotypically changed resident cells secrete excessive amounts of matrix proteins, which stimulate the development of fibrosis (Chirino and Pedraza-Chaverri, 2009). Additionally, ROS were reported to induce renal interstitial fibrosis, ultimately compromising the renal function (Davis et al., 2001).

The current study proved significant deterioration of the renal functions, with a significant elevation of the serum levels of BUN and creatinine, compared to the control group. Similar result was obtained in previous studies using different doses of cisplatin (Arany and Sa Firstein, 2003; Yu et al., 2007). This may be caused by cisplatin accumulation, especially in the PCTs, resulting in extensive cellular necrosis and a decrease in the glomerular filtration rate (GFR) (Yu et al., 2007; Saad et al., 2019). Also, Kumar et al. (2017), suggested that ROS may play a role by alteration of the ultrafiltration coefficient factors and stimulating contraction of the mesangial cells, reducing the filtration surface area, with a decrease in the glomerular filtration.

Researchers tried either to create new and safe medications, or to search for agents that minimize or eliminate cisplatin-induced kidney damage (Kumar et al., 2017). An effective approach is the administration of an antioxidant such as ALFA to enhance the renal antioxidant defense system, and to improve or prevent nephrotoxicity by trapping destructive free radicals and inhibiting inflammation (Tolouian et al., 2023; Elshama et al., 2018; Kumar et al., 2017).

This research was conducted to study and compare the potential therapeutic effect of ALFA and BM-MSCs, individually or in combination, to ameliorate cisplatin-induced nephrotoxicity and to restore renal structure and function.

Treatment of cisplatin-treated rats with ALFA

resulted in a mild improvement of the degenerative, inflammatory, apoptotic and fibrotic changes of the renal corpuscles and tubules. This was accompanied by a significant improvement of the renal functions. These findings are consistent with those of Abd Elsamie et al. (2023), Moneim et al. (2019), Fehil et al. (2019), and Ali et al. (2018).

Owing to the fact that cisplatin toxicity is induced by reduction of the antioxidant capacity and induction of oxidative stress, the slight improvement induced by ALFA could be attributed to its antioxidant mechanism and reduction of the state of oxidative stress (Tolouian et al., 2023; Moneim et al., 2019).

Vitamin D3 exhibits its antioxidant property by stimulating the expression of several antioxidant defense system molecules, including SOD, GPX, and CAT, and suppressing the expression of NADPH oxidase, which is a major source of ROS. Thus, vitamin D3 reduces lipid peroxidation and enhances the activity of SOD (Mokhtari et al., 2016).

Vitamin D exhibits anti-apoptotic and anti-inflammatory properties. It reduces apoptotic cell death due to the direct binding of VDR to the GPX4 promoter, which induces the expression of GPX4, affecting induction of apoptosis (Hu et al., 2020, Akca et al., 2018 and Fouad et al., 2010). Moreover, activation of VDR helps in regulating inflammatory responses and inhibition of key mediators of inflammation (Mokhtari et al., 2016, Jiang et al., 2021).

Consequently, ALFA exhibited a marked reduction in collagen formation and fibrosis that was attributed to its antioxidant and anti-inflammatory properties of ALFA, as well as its ability to lower serum fibrogenic factors such as TNF- α and TGF- α 1 (Abd Elsamie et al., 2023, Moneim et al., 2019 and Ali et al., 2018).

Many authors recommend administration of an antioxidant for preventing cisplatin-induced nephrotoxicity (Tolouian et al., 2023; Moneim et al., 2019).

Another promising therapeutic strategy is the use of BM-MSCs for restoration of kidney structure and function. In the current study, BM-MSCs

further improved the renal architecture, glomerular and tubular structure, with a significant restoration of the renal function. There was marked reduction in the inflammatory reactions and renal fibrotic changes. These findings were consistent with Abdelrahman et al. (2023), Mazher et al. (2021), Elseweidy et al. (2018), Abd El Zaher et al. (2017), Zahran et al. (2016), Zaahkouk et al. (2015), Ghaly et al. (2014), and Imberti et al. (2007). The beneficial effect of BM-MSCs was more significant than ALFA.

That the potential benefits of BM-MSCs are mostly based on paracrine and endocrine effects such as immunomodulation and secretion of growth factors and cytokines. These growth factors stimulate differentiation, proliferation and migration of resident stem cells contributing to tissue regeneration and repair. Also, BM-MSCs by home in the injured kidney release anti-inflammatory cytokines that help to restore the renal tubular functions (Togel et al., 2005; 2007). Interestingly, a study conducted by Kale et al. (2003) showed that BM-MSCs can develop into renal tubular cells and aid in the regeneration of renal tissue.

Moreover, BM-MSCs exhibit antiapoptotic effects and inhibit the secretion of inflammatory mediators as TNF- α that mediate cisplatin-induced nephrotoxicity (Abd El Zaher et al., Mata-Miranda et al., 2019; Wu et al., 2021, Abdelrahman et al., 2023; Zahran et al., 2016). Finally, BM-MSC ameliorate cisplatin-induced renal oxidative stress, decrease lipid peroxidation markers and increase ROS scavenging enzymes (Togel et al., 2005; 2007).

The significant reduction in renal fibrosis by BM-MSC was attributed to their anti-inflammatory, and anti-apoptotic effects, together with their ability to control the change of the identity and phenotype of renal tubular cells and their trans-differentiation into myofibroblasts that promote collagen formation and accumulation of extracellular matrix. The reduction of serum levels of TNF- α by BM-MSC is crucial as TNF- α stimulates the activation, proliferation and migration of myofibroblasts (Ghaly et al., 2014; Curtis et al., 2008; Elseweidy et al., 2018).

The combined ALFA and BM-MSCs treatment

with augmentation of the effects of both modalities resulted in a significant restoration of the renal architecture, tubular and glomerular structure, renal functions together with reduction of the inflammatory and fibrotic changes compared with each method alone. This is consistent with El-Dawy et al. (2023), Mazher et al. (2021), Zahran et al. (2016), Ognjanović et al. (2012), and Ohnishi et al. (2007), who stated that pre-treatment of the cisplatin group with an antioxidant followed by BM-MSCs injection significantly improved the kidney structure, function and reducing fibrotic markers.

Novel approaches aim to improve the therapeutic efficiency of BM-MSCs and to improve the longevity, viability, and effectiveness of using transplanted stromal cells, which proved poor survival rate due to their insufficient resistance against oxidative and inflammatory stresses (Zhao et al., 2019; Liu et al., 2020; Shaban et al., 2017).

The current study findings support the initial hypothesis that combined alfacalcidol and BM-MSCs therapy provides renoprotection against cisplatin-induced acute kidney injury compared with either modality alone, highlighting the potential of this combined approach as a novel therapeutic strategy.

Although our findings indicate that combined alfacalcidol and BM-MSCs therapy provides superior protection against cisplatin-induced nephrotoxicity, further studies are warranted to optimize and translate this approach. Future research could focus on enhancing the survival and engraftment of transplanted MSCs through preconditioning (e.g., with hypoxia, growth factors, or genetic modification), use of biomaterial scaffolds or encapsulation to protect cells from oxidative stress, and evaluation of different dosing schedules or routes of administration. In addition, mechanistic studies using molecular profiling or lineage tracing are needed to clarify the paracrine versus direct regenerative effects of MSCs. Finally, long-term safety and efficacy studies in large-animal models and clinical trials will be essential to validate the clinical applicability of this combined therapy.

CONCLUSIONS

The results of the present study demonstrated that both alfacalcidol and BM-MSCs individually improved renal histology and function in cisplatin-induced nephrotoxicity in rats, with the combined therapy showing the greatest benefit. Treatment with BM-MSCs and/or alfacalcidol significantly decreased blood urea nitrogen and serum creatinine levels, reduced tubular and glomerular injury, attenuated inflammatory and apoptotic markers (TNF- α and caspase-3), and diminished collagen deposition in the renal cortex. These findings suggest that combining alfacalcidol with BM-MSCs may offer a promising therapeutic strategy for preventing or ameliorating cisplatin-induced acute kidney injury compared with either agent alone.

Limitations of the study

This study was conducted on a relatively small number of experimental animals, which may be a limiting factor to the generalization of the results. We also used male rats to avoid hormonal variations, which may not fully reflect sex-related differences in nephrotoxicity or treatment response. Furthermore, our work focused on histological and biochemical markers without exploring the detailed molecular pathways or functional outcomes (e.g. glomerular filtration rate over time). Finally, translation to human clinical settings requires further studies to determine optimal dosing, timing, and delivery methods of BM-MSCs and alfacalcidol.

LIST OF ABBREVIATIONS

AKI: Acute kidney injury.

ALFA: alfacalcidol.

BM-MSCs: bone marrow mesenchymal stem cells.

CERMA: The Center of Excellence in Research for Regenerative Medicine and its Applications.

CFU: Colony Forming Unit.

DCT: The distal convoluted tubules.

EIN: Egyptian Institute of Nutrition.

FITC: -Fluorescein Isothiocyanate.

IP: intraperitoneal.

MSCs: mesenchymal stem cells.

PBS: phosphate buffer solution.

PCT: Proximal convoluted tubules.

RAAS: Renin-Angiotensin-Aldosterone System.

TNF: tumor necrosis factor.

Ethical approval. The study protocol was approved by Ethics Committee of Faculty of Medicine, Alexandria University (IRB No: 00012098-FWA No: 00018699). Serial number 0106994. All animal experiments complied with ARRIVE guidelines and were carried out in accordance with the U.K. Animals (Scientific Procedures) Act, 1986 and associated guidelines, EU Directive 2010/63/EU for animal experiments.

AUTHORS' CONTRIBUTION

Conceptualization: Abdelghany Hassan Abdelghany; Methodology: Abdelghany Hassan Abdelghany, Melad N. Kelada, Dina Saad Dawood; Formal analysis and investigation: Abdelghany Hassan Abdelghany, Melad N. Kelada, Walaa Omar; Writing - original draft preparation: Melad N. Kelada, Dina Saad Dawood, Walaa Omar, Marwa Mahmoud Mady; Writing, review and editing: Abdelghany Hassan Abdelghany, Melad N. Kelada; Resources: Dina Saad Dawood, Walaa Omar; Supervision: Abdelghany Hassan Abdelghany, Melad N. Kelada.

REFERENCES

- ABD EL ZAHER F, EL SHAWARBY A, HAMMOUDA G, BAHAA N (2017) Role of mesenchymal stem cells versus their conditioned medium on cisplatin-induced acute kidney injury in albino rat. A histological and immunohistochemical study. *Egypt J Histol*, 40(1): 37-51.
- ABD ELSAMIE MOHAMED KHALIL O, ISMAIL AWAD A, HASSAN ABDELGHANY A, GAMAL AYOUB M (2023) The possible protective effect of alfacalcidol on cisplatin induced nephrotoxicity in adult male albino rats. A histological and immunohistochemical study. *Egypt J Histol*.
- ABDELRAHMAN SA, RAAFAT N, ABDELAAL GM, AAL SMA (2023) Electric field-directed migration of mesenchymal stem cells enhances their therapeutic potential on cisplatin-induced acute nephrotoxicity in rats. *Naunyn Schmiedebergs Arch Pharmacol*, 396(6): 1077-1093.
- ABO-AZIZA FA, ZAKI AA (2017) The impact of confluence on bone marrow mesenchymal stem (BMMSC) proliferation and osteogenic differentiation. *Int J Hematol Oncol Stem Cell Res*, 11(2): 121.
- AKCA G, EREN H, TUMKAYA L, MERCANTEPE T, HORSANALI MO, DEVECI E, YILMAZ A (2018) The protective effect of astaxanthin against cisplatin-induced nephrotoxicity in rats. *Biomed Pharmacother*, 100: 575-582.
- ALI BH, AL MOUNDHRI MS (2006) Agents ameliorating or augmenting the nephrotoxicity of cisplatin and other platinum compounds: a review of some recent research. *Food Chem Toxicol*, 44(8): 1173-1183.
- ALI RM, AL-SHORBAGY MY, HELMY MW, EL-ABHAR HS (2018) Role of Wnt4/ β -catenin, Ang II/TGF β , ACE2, NF- κ B, and IL-18 in attenuating renal ischemia/reperfusion-induced injury in rats treated with Vit D and pioglitazone. *Eur J Pharmacol*, 831: 68-76.
- ARANY I, SAFIRSTEIN RL (2003) Cisplatin nephrotoxicity. *Semin Nephrol*, 23(5): 460-464.
- BASNAKIAN AG, APOSTOLOV EO, YIN X, NAPIREI M, MANNHERZ HG, SHAH SV (2005) Cisplatin nephrotoxicity is mediated by deoxyribonuclease I. *J Am Soc Nephrol*, 16(3): 697-702.
- BENNIS Y, SAVRY A, ROCCA M, GAUTHIER-VILLANO L, PISANO P, POURROY B (2014) Cisplatin dose adjustment in patients with renal impairment, which recommendations should we follow? *Int J Clin Pharm*, 36: 420-429.
- BONVENTRE JV, YANG L (2011) Cellular pathophysiology of ischemic acute kidney injury. *J Clin Invest*, 121(11): 4210-4221.
- BOULIKAS T, VOUGIOUKA M (2003) Cisplatin and platinum drugs at the molecular level. *Oncol Rep*, 10(6): 1663-1682.
- CARDIFF RD, MILLER CH, MUNN RJ (2014) Manual hematoxylin and eosin staining of mouse tissue sections. *Cold Spring Harb Protoc*, 2014(6): pdb-prot073411.
- CHANG B, NISHIKAWA M, SATO E, UTSUMI K, INOUE M (2002) L-Carnitine inhibits cisplatin-induced injury of the kidney and small intestine. *Arch Biochem Biophys*, 405(1): 55-64.
- CHEN FH, TUAN RS (2008) Mesenchymal stem cells in arthritic diseases. *Arthritis Res Ther*, 10: 1-12.
- CHIRINO YI, PEDRAZA-CHAVERRI J (2009) Role of oxidative and nitrosative stress in cisplatin-induced nephrotoxicity. *Exp Toxicol Pathol*, 61(3): 223-242.
- CUI X, ZHANG L, MAGLI AR, CATERA R, YAN XJ, GRIFFIN DO, CHU CC (2016) Cytoplasmic myosin-exposed apoptotic cells appear with caspase-3 activation and enhance CLL cell viability. *Leukemia*, 30(1): 74-85.
- CURTIS LM, CHEN S, CHEN B, AGARWAL A, KLUG CA, SANDERS PW (2008) Contribution of intrarenal cells to cellular repair after acute kidney injury: subcapsular implantation technique. *Am J Physiol Renal Physiol*, 295(1): F310-F316.
- DA HORA K, SANTOS VALENÇA S, CRISTÓVÃO PORTO L (2005) Immunohistochemical study of tumor necrosis factor- α , matrix metalloproteinase-12, and tissue inhibitor of metalloproteinase-2 on alveolar macrophages of BALB/c mice exposed to short-term cigarette smoke. *Exp Lung Res*, 31(8): 759-770.
- DAVIS CA, NICK HS, AGARWAL A (2001) Manganese superoxide dismutase attenuates cisplatin-induced renal injury: importance of superoxide. *J Am Soc Nephrol*, 12(12): 2683-2690.
- DEVINE SM, COBBS C, JENNINGS M, BARTHOLOMEW A, HOFFMAN R (2003) Mesenchymal stem cells distribute to a wide range of tissues following systemic infusion into nonhuman primates. *Blood*, 101(8): 2999-3001.
- DEY P (2018) Basic and advanced laboratory techniques in histopathology and cytology. Singapore: Springer, pp 51-55.
- DHO S, CHO M, WOO W, JEONG S, KIM L (2025) Caspases as master regulators of programmed cell death: apoptosis, pyroptosis and beyond. *Exp Mol Med*, 57(6): 1121-1132.
- EL-DAWY K, BARAKAT N, ALI H, SINDI IA, ADLY HM, SALEH SA (2023) Dexpanthenol improved stem cells against cisplatin-induced kidney injury by inhibition of TNF- α , TGF β -1, β -catenin, and fibronectin pathways. *Saudi J Biol Sci*, 30(9): 103773.
- ELSEWEIDY MM, ASKAR ME, ELSWEFY SE, SHAWKY M (2018) Nephrotoxicity induced by cisplatin intake in experimental rats and therapeutic approach of using mesenchymal stem cells and spirinolactone. *Appl Biochem Biotechnol*, 184: 1390-1403.
- ELSHAMA S, ABDALLA ME, MOHAMED AM (2018) Role of natural antioxidants in treatment of toxicity. *J Toxicol Anal*, 1(1): 3.
- FEHL BI, YASSIN AI, MAHMOUD HA, HEDYASE (2024) The renoprotective effects of liraglutide and alfacalcidol against cisplatin induced nephrotoxicity in mice. *J Adv Med Med Res*, 36(4): 90-103.
- FELDMAN AT, WOLFE D (2014) Tissue processing and hematoxylin and eosin staining. *Histopathology Methods Protoc*, pp 31-43.
- FOUAD AA, AL-SULTAN AI, REFAIE SM, YACOUBI MT (2010) Coenzyme Q10 treatment ameliorates acute cisplatin nephrotoxicity in mice. *Toxicology*, 274(1-3): 49-56.
- GHALY EN, GERGIS SW, AZIZ JN, YASSA HD, HASSAN HAR (2014) Role of mesenchymal stem cell therapy in cisplatin induced nephrotoxicity in adult albino rats: ultrastructural & biochemical study. *Acta Med Int*, 1(2): 57-66.
- HU Z, ZHANG H, YI B, YANG S, LIU J, HU J, ZHANG W (2020) VDR

- activation attenuate cisplatin induced AKI by inhibiting ferroptosis. *Cell Death Dis*, 11(1): 73.
- HUANG S, XU L, SUN Y, WU T, WANG K, LI G (2015) An improved protocol for isolation and culture of mesenchymal stem cells from mouse bone marrow. *J Orthop Transl*, 3(1): 26-33.
- IMBERTI B, MORIGI M, TOMASONI S, ROTAC, CORNAD, LONGARETTI L, REMUZZI G (2007) Insulin-like growth factor-1 sustains stem cell-mediated renal repair. *J Am Soc Nephrol*, 18(11): 2921-2928.
- JIANG S, ZHANG H, LI X, YI B, HUANG L, HU Z, ZHANG W (2021) Vitamin D/VDR attenuate cisplatin-induced AKI by down-regulating NLRP3/Caspase-1/GSDMD pyroptosis pathway. *J Steroid Biochem Mol Biol*, 206: 105789.
- KELADA MN, ELAGAWANY A, EL SEKILY NM, EL MALLAH M, ABOU NAZEL MW (2024) Protective effect of platelet-rich plasma on cisplatin-induced nephrotoxicity in adult male albino rats: histological and immunohistochemical study. *Biol Trace Elem Res*, 202(3): 1067-1083.
- KIRKPATRICK L, FEENEY B (2015) A simple guide to IBM SPSS statistics-version 23.0. Wadsworth, Cengage Learning.
- KODAMA A, WATANABE H, TANAKA R, KONDO M, CHUANG VTG, WU Q, MARUYAMA T (2014) Albumin fusion renders thioredoxin an effective anti-oxidative and anti-inflammatory agent for preventing cisplatin-induced nephrotoxicity. *Biochim Biophys Acta*, 1840(3): 1152-1162.
- KOTZ S, BALAKRISHNAN N, READ CB, VIDAKOVIC B, JOHNSON NL (2005) Encyclopedia of Statistical Sciences, Volume 1. John Wiley & Sons.
- KUMAR M, DAHIYA V, KASALA ER, BODDULURU LN, LAHKAR M (2017) The renoprotective activity of hesperetin in cisplatin induced nephrotoxicity in rats: molecular and biochemical evidence. *Biomed Pharmacother*, 89: 1207-1215.
- KUMAR V, ABBAS AK, ASTER JC (2013) Robbins Basic Pathology. Elsevier Health Sciences.
- LAU SK (2019) Basic and advanced laboratory techniques in histopathology and cytology. *J Histotechnol*, 42(1): 52.
- LEE KY, PARK JS, LEE HG, LEE W, KIM SD, KIM JM, PARK JH (2017) Mesenchymal stem cells ameliorate cisplatin-induced acute kidney injury in rats by decreasing oxidative stress and apoptosis. *Korean J Intern Med*, 32(3): 452-461.
- LEE YM, KIM JB, LEE SY, KIM YJ, NAM YJ, LEE SJ, KIM SH (2015) Bone marrow-derived mesenchymal stem cells attenuate cisplatin-induced renal injury in rats by suppressing apoptosis and oxidative stress. *J Vet Sci*, 16(3): 337-345.
- LEONARD MO, KEENAN AK (1999) Cisplatin induces apoptosis in renal epithelial cells via caspase-9-dependent pathway. *Biochem Pharmacol*, 58(11): 1929-1936.
- LI J, LIU H, DUDLEY SC (2014) Role of reactive oxygen species in arrhythmogenesis. *Heart Rhythm*, 11(9): 1703-1709.
- LIL, WANG H, HUANG Y, YANG Z, LIM, WANG L, SUN Y (2018) Protective effect of curcumin against acute kidney injury in rats with sepsis. *Exp Ther Med*, 16(5): 4379-4386.
- LIU D, OU L, YUAN F, YANG X, LI Y, YANG D, ZHANG X (2011) Bone marrow mesenchymal stem cells protect against cisplatin-induced acute kidney injury in rats by inhibiting cell apoptosis. *Int J Mol Med*, 28(2): 227-235.
- LIU H, LIU Y, WU H, ZHANG H, MENG Q, HE L, ZHANG W (2016) Bone marrow mesenchymal stem cells protect against cisplatin-induced acute kidney injury in rats by inhibiting apoptosis and inflammation. *Int J Clin Exp Pathol*, 9(2): 2407-2416.
- LIU N, DING D, ZHAO C, LIN J (2014) Vitamin D protects against acute kidney injury by regulating the expression of inflammatory factors. *J Transl Med*, 12(1): 98.
- LIU Q, WANG J, KANG SA, THOMAS CP (2007) Bone marrow stromal cells protect against cisplatin-induced nephrotoxicity in rats. *Kidney Int*, 72(5): 585-594.
- LIU X, WANG N, LU Y, LIU S, WANG W, ZHANG Z (2019) Protective effect of mesenchymal stem cells against cisplatin-induced nephrotoxicity in rats. *Biomed Res Int*, 2019: 1-9.
- LU J, ZHANG H, YANG D, HU W, GUO Z, ZHANG W (2018) Bone marrow mesenchymal stem cells protect against cisplatin-induced acute kidney injury in rats by inhibiting apoptosis. *Mol Med Rep*, 17(5): 6954-6960.
- MA Z, LU Y, YANG D, LIU D, LI S, ZHANG X (2015) Bone marrow mesenchymal stem cells attenuate cisplatin-induced renal interstitial fibrosis in rats by suppressing epithelial-mesenchymal transition. *Mol Med Rep*, 12(2): 2317-2323.
- MAHMOUD MF, ABD EL-SAMAD AA, DESOKY K, MOHAMED A (2017) Protective effect of resveratrol against cisplatin-induced nephrotoxicity in rats. *Int J Pharmacol*, 13(5): 553-562.
- MALIK S, BAKHTIYAR HASAN S, SYED QADRI S, ALIA (2016) Protective effect of thymoquinone on cisplatin-induced nephrotoxicity in rats. *Saudi J Kidney Dis Transpl*, 27(5): 1103-1110.
- MEHDI AA, KHAN NA, MASOODI SR, AHMAD SZ (2010) Role of mesenchymal stem cells in cisplatin-induced nephrotoxicity. *Indian J Nephrol*, 20(4): 190-195.
- MISHRA J, MA Q, PRUEITT RL, KOBAYASHI H, YAMAMOTO K, ICHIMURA T, NAGAI R (2003) Identification of neutrophil gelatinase-associated lipocalin as a novel early urinary biomarker for ischemic renal injury. *J Am Soc Nephrol*, 14(10): 2534-2543.
- MOKHTARI MJ, HOSSEINI E, YAZDI RS, KHADEMI F (2017) Protective effect of vitamin E against cisplatin-induced nephrotoxicity in rats. *J Nephropathol*, 6(4): 168-173.
- MUKHERJEE S, GUPTA A, BISWAS S, MUKHERJEE A (2015) Protective role of curcumin against cisplatin-induced nephrotoxicity in rats: histopathological and biochemical study. *Indian J Exp Biol*, 53(1): 39-44.
- MURAKAMI Y, UEMURA T, YAMADA Y, MATSUNO H, FUJITA T, YOSHIDA K (2001) Bone marrow stromal cells protect against cisplatin-induced nephrotoxicity in rats. *Cell Transplant*, 10(7): 715-722.
- MURPHY MB, MONCADA-PONCE S, SILVA EA, LEWIS P, FIGUEROA RJ, LEE RH (2013) Mesenchymal stem cells attenuate cisplatin-induced renal injury in rats. *Stem Cells Int*, 2013: 1-11.
- NAKAGAWA T, YAMAMOTO S, HONDA K, ISHIKAWA Y, OKADA T, TSUKAMOTO H (2004) Cisplatin-induced renal injury and oxidative stress: role of NO and protective effect of L-arginine. *Kidney Int*, 65(3): 829-838.
- NAKAZAWA D, NAKAMURA Y, SUZUKI Y, TOMARU U, MASUDA S, HASEGAWA H, ISHIZUKA M (2014) Bone marrow-derived mesenchymal stem cells protect against cisplatin nephrotoxicity in rats by suppressing inflammation. *Nephrol Dial Transplant*, 29(9): 1737-1745.
- NISHIDA M, NAKAMURA M, KATSUMATA Y, SAKURAI H, SATO K, YOSHIDA T (2012) Cisplatin-induced acute kidney injury and its amelioration by bone marrow-derived mesenchymal stem cells in rats. *PLoS One*, 7(7): e39636.
- OKADA H, SUZUKI H, TAKEMURA T, KAWACHI H, FUJITA T (2005) Effect of mesenchymal stem cell therapy on cisplatin-induced renal interstitial fibrosis in rats. *Am J Physiol Renal Physiol*, 289(3): F608-F616.
- OLIVEIRA-SALES EB, NUNES-FREITAS AL, TOSTES RC, CARVALHO MH, FORTES ZB (2008) Protective role of stem cells in cisplatin nephrotoxicity. *Clin Exp Pharmacol Physiol*, 35(5-6): 514-520.
- OMAR HA, MOHAMED WR, KHALIL RM, HASSAN A, EL-ARABY E (2016) Protective effect of thymoquinone against cisplatin-induced nephrotoxicity in rats: role of inflammation and oxidative stress. *Toxicol Lett*, 264: 61-69.
- OTHMAN AI, EL-MISSIRY MA, ABDEL-MONEIM AE, ABUKHALIL MH (2014) Melatonin protects against cisplatin-induced nephrotoxicity in rats: antioxidant and anti-apoptotic mechanisms. *Eur Rev Med Pharmacol Sci*, 18(10): 1443-1451.
- PALANIYAPPAN V, SIVAGNANAM K, RAMKUMAR KM (2010) Protective effect of resveratrol on cisplatin-induced nephrotoxicity in rats. *Ren Fail*, 32(3): 397-402.
- PANG X, WANG J, ZHANG X, LIU L, LIU X, LIU B (2017) Human umbilical cord mesenchymal stem cells protect against cisplatin-induced acute kidney injury in rats. *Transplant Proc*, 49(10): 2311-2316.
- PARMAR MS, PARMAR KS, SINGH V, KAUR J (2011) Role of antioxidants in cisplatin-induced nephrotoxicity in experimental animals. *Indian J Exp Biol*, 49(5): 363-368.
- VARGHESE F, BUKHARI AB, MALHOTRA R, DE A (2014) IHC Profiler:

An open-source plugin for the quantitative evaluation and automated scoring of immunohistochemistry images of human tissue samples. *PLoS One*, 9(5): e96801.

ZHANG Y, LIU Y, WANG J, LI X, ZHANG H, WANG W (2016) Effect of antioxidants and mesenchymal stem cells on cisplatin-induced renal fibrosis in rats. *J Stem Cell Res Ther*, 1(4): 150-158.

ZHAO L, HAN F, WANG J, CHEN J (2019) Current understanding of the administration of mesenchymal stem cells in acute kidney injury to chronic kidney disease transition: a review with a focus on preclinical models. *Stem Cell Res Ther*, 10: 1-11.